Journal of Power Sources 195 (2010) 3431–3450

Contents lists available at ScienceDirect

Journal of Power Sources

journal homepage: www.elsevier.com/locate/jpowsour

Alkaline direct alcohol fuel cells

E. Antolini[a,b,*], E.R. Gonzalez[b]

[a] Scuola di Scienza dei Materiali, Via 25 aprile 22, 16016 Cogoleto, Genova, Italy
[b] Instituto de Química de São Carlos, USP, C. P. 780, São Carlos, SP 13560-970, Brazil

ARTICLE INFO

Article history:
Received 14 September 2009
Received in revised form
24 November 2009
Accepted 27 November 2009
Available online 6 January 2010

Keywords:
Alcohol oxidation
Oxygen reduction
Anion-exchange membranes
Direct alcohol fuel cells
Electrocatalysts

ABSTRACT

The faster kinetics of the alcohol oxidation and oxygen reduction reactions in alkaline direct alcohol fuel cells (ADAFCs), opening up the possibility of using less expensive metal catalysts, as silver, nickel and palladium, makes the alkaline direct alcohol fuel cell a potentially low cost technology compared to acid direct alcohol fuel cell technology, which employs platinum catalysts. A boost in the research regarding alkaline fuel cells, fuelled with hydrogen or alcohols, was due to the development of alkaline anion-exchange membranes, which allows the overcoming of the problem of the progressive carbonation of the alkaline electrolyte. This paper presents an overview of catalysts and membranes for ADAFCs, and of testing of ADAFCs, fuelled with methanol, ethanol and ethylene glycol, formed by these materials.
© 2009 Elsevier B.V. All rights reserved.

1. Introduction

Among different types of fuel cells, alkaline fuel cells (AFCs) are the most matured. The AFCs were developed and studied extensively throughout the 1960s to the 1980s [1]. Since then, AFCs have lost their popularity to other new emerging fuel cell technologies such as the proton-exchange membrane fuel cell (PEMFC) because of the flexibility of using a solid electrolyte and the avoidance of electrolyte leakage. However, comparison between AFC and PEMFC [2] indicated that AFCs can theoretically outperform PEMFCs and some of the earliest pressurized AFC systems showed current densities much higher than those achieved today with current PEM technology. Ambient air operated AFCs produce current densities comparable to ambient air operated PEMFCs. Cost analysis showed that AFC systems for low power applications including hybrid vehicles are at least competitive with the cost of any equivalent system constructed using PEMFC technology [2]. Alkaline fuel cells have numerous advantages over proton exchange membrane fuel cells on both cathode kinetics and ohmic polarization. The less-corrosive nature of an alkaline environment ensures a potential greater longevity. The kinetics of the ORR reaction is more facile in alkaline medium than in some acid medium such as H_2SO_4 using Pt catalysts [3] and $HClO_4$ using Ag catalysts [4]. The inherently faster kinetics of the oxygen reduction reaction in an alkaline fuel cell allows the use of non-noble and low-cost metal electrocatalysts such as silver and nickel, making the AFC a potentially low cost technology compared to PEMFCs, which employ platinum catalysts. Thus, a resurgence of interest in AFCs has occurred in recent years [5–9]. A serious problem of AFCs was the progressive carbonation of the alkaline electrolyte due to CO_2 from air or the oxidation product of the fuel, addressed mainly by the application of alkaline anion exchange membranes (AAEMs) [10–12]. Indeed, a boost in the research regarding AFC is related to the development of alkaline anion-exchange membranes. Alkaline fuel cells using AAEMs have several important advantages over conventional AFCs: (i) since there is no mobile cation, there is no precipitated carbonate, (ii) no electrolyte weeping, (iii) reduced alcohol crossover, (iv) potentially simplified water management, due to the fact that the water is produced at the anode and consumed at the cathode, and (v) potentially reduced corrosion [13].

The development of alternative power sources is an important issue at present. Direct alcohol fuel cells (DAFCs) have attracted considerable interest in their application to alternative power sources for automobile and portable consumer electronics [14]. Liquid fuels, such as low-molecular weight alcohols, have several advantages compared to pure hydrogen, because they can be easy handled, stored and transported. Furthermore, they have relatively high mass energy density, comparable to that of gasoline. Methanol is a promising fuel for DAFCs [15], but other low molecular weight alcohols such as ethanol [16] and ethylene glycol [17] are also candidates. At present, DAFCs are mostly using acidic proton exchange membrane. With strong acidic electrolyte membrane, CO_2 generated in anodic reaction can be easy removed. A major contribution

* Corresponding author at: Scuola di Scienza dei Materiali, Via 25 aprile 22, 16016 Cogoleto, Genova, Italy.
E-mail address: ermantol@libero.it (E. Antolini).

0378-7753/$ – see front matter © 2009 Elsevier B.V. All rights reserved.
doi:10.1016/j.jpowsour.2009.11.145

to the relatively low DAFC performance is from kinetic constraints in the alcohol oxidation reaction in acid media. Improved alcohol oxidation kinetics can be facilitated using basic media [18]. In addition, the ionic current in alkali fuel cells is due to conduction of hydroxide ions and is the reverse direction to that in proton conducting systems. As such, the direction of the electro-osmotic drag is reversed, reducing the alcohol permeation rate [19]. Accordingly, the approach is to develop an alkali analogue of the DAFC. The recent development of polymeric membrane presenting a good anionic conductivity opens a new research area to conceive solid fuel cells working with an electrolytic membrane different from the common proton exchange membrane. Several DAFCs which use an alkaline anion exchange membrane as a polymer electrolyte membrane have already been reported [10,19–21]. An advantage of using alkaline fuel cells, rather than the traditional acidic fuel cells, is the potential use of non-Pt catalysts in the electrodes. The development of new anode and cathode catalyst systems is more likely in alkaline media because of the wide range of options for the materials support and catalyst, as compared to acidic media which offers more limited materials choice. Alternatives to platinum have been investigated, showing good performance, comparable sometimes to platinum itself.

This paper presents an overview of catalyst and membranes for alkaline direct alcohol fuel cells, and reports the testing of these materials in alkaline direct alcohol fuel cells fuelled with C_1 (methanol) and C_2 (ethanol and ethylene glycol) alcohols. In literature alkaline fuel cells using an alcohol as the fuel are named both alkaline direct alcohol fuel cells (ADAFC) and direct alcohol alkaline fuel cells (DAAFC). In this work we always will used the former expression, to avoid misunderstandings with the acronym of the direct ascorbic acid fuel cell, DAAFC.

2. Anode catalysts

2.1. Catalysts for methanol oxidation in alkaline media.

The use of alkali electrolytes not only lead to better polarization characteristics of methanol oxidation on platinum compared to acid media, but also open up the possibility of using non-noble, less expensive metal catalysts for the process.

2.1.1. Pt and Pt-based catalysts

Platinum has the highest catalytic activity for the methanol oxidation reaction (MOR) of any of the pure metals both in acid and in alkaline media. An excellent review on the MOR on Pt and Pt-based catalysts in alkaline media was done by Spendelow and Wieckowski [22]. Concisely, the enhanced activity in alkaline media results from at least two factors: the lack of specifically-adsorbing spectator ions in alkaline solutions, and the higher coverage of adsorbed OH at low potential, which is required for methanol oxidation [22].

The rate limiting step during the MOR on Pt in alkaline media is a chemical step involving reaction of adsorbed MOR intermediates (such as CO or CHO) and adsorbed OH [23]. The final product of the MOR in alkaline media, carbonate or formate, is a subject of some controversy. Tripkovic et al. [24] carried out a comparative study of methanol oxidation on a Pt(1 0 0) surface in various alkaline solutions. They found that Pt(1 0 0) adsorbs OH and 'poisoning species'. The 'poisoning species', produced in methanol oxidation, participate in the reaction at higher potentials, but block the surface partially at lower potentials. A dual path reaction mechanism, common to all the alkaline solutions used, was proposed based on the assumptions that HCO is a reactive intermediate and that a formate is a reaction product in the main path, while CO_2 is a product of 'poisoning species' oxidation in a parallel reaction path. Tripkovic et al. [25] performed the electrochemical oxidation of methanol, ethanol, *n*-propanol and *n*-butanol at the Pt(1 1 1). They observed that reversible OH_{ad} species were produced in a fast process of OH^- adsorption as opposite to irreversible OH_{ad} species, which could be generated only during a time-dependent adsorption. The reversibly adsorbed OH species are the active intermediates in alcohol oxidation, while the irreversible adsorbed OH species are the inactive, strongly bound intermediates, acting as a 'poison' in the alcohol oxidation. Spendelow and Wieckowski [22] concluded that the different final reaction products reported in the literature for the MOR on Pt(1 1 1) simply reflect the different potential ranges in which the MOR is examined.

A lot of papers have been addressed to the methanol oxidation on Pt-Ru catalyst in acidic media, and excellent reviews have been done by Spendelow et al. [26] and Petrii [27]. Conversely, few works have been addressed to the MOR on Pt-Ru catalysts in alkali media. Firstly, Petrii et al. [28] compared the polarization curves of methanol electro-oxidation in an alkaline solution under steady state conditions on Pt-Ru (Pt:Ru atomic ratio 9:1) deposited on platinum with those on a platinized-platinum electrode. They found that the overvoltage of methanol oxidation on Pt-Ru is 60-70 mV lower than on Pt/Pt at a current density of 2.5 mA cm^{-2}. Rauhe et al. [29] performed methanol electro-oxidation on poor alloyed Pt-Ru (1:1) in Cs_2CO_3 electrolytes at 100–140 °C and ambient pressures. They found that Pt-Ru/C provided enhanced performance, compared to Pt/C. Performance curves, based on unit catalyst mass, for Pt-Ru/C at 120 °C matched or exceeded previously reported performance data for supported Pt or Pt black in concentrated Cs_2CO_3 electrolytes at 120–150 °C at 8 atm, and for supported Pt-Ru in concentrated H_3PO_4 electrolytes at 200 °C. Tripkovic et al. [18,30] investigated the kinetics of methanol oxidation on supported Pt and Pt-Ru (Pt:Ru = 3:2 and 2:3) catalysts in 0.5 M H_2SO_4 and 0.1 NaOH at 22 and 60 °C. At room temperature, the Pt-Ru catalysts were slightly more active than Pt for methanol oxidation in alkaline solution, suggesting a promoter effect of Ru on OH^- adsorption. Higher activity of Pt_3Ru_2 than Pt_2Ru_3 catalyst was observed, ascribed to the higher rate of methanol dehydrogenation/adsorption on Ru-less rich alloy. At higher temperatures, a negligible difference in the kinetics between Pt and Pt-Ru catalysts was observed. Jayashree et al. [31] compared the performance of an air-breathing laminar flow-based direct methanol fuel cell (LFFC) operated in acidic or alkaline media at room temperature with a bulk Pt-Ru (1:1) alloy as the anode catalyst. Fig. 1 from ref. [31] shows polarization and power density curves for the LFFCs operated in acidic and alkaline media under identical operating conditions. As can be seen in Fig. 1, the performance of LFFCs operated in alkaline media was higher than that of LFFCs in acidic media. A maximum power density of 11.8 and 17.2 mW cm^{-2} was found for operation in acidic and alkaline media, respectively.

Besides Ru, a variety of alloyed metals, metal ad-atoms and metal oxides have been investigated as MOR promoters on Pt in alkaline media. Kadirgan et al. [32] investigated the electrocatalytic oxidation of methanol on Pt–Pd alloy electrodes of different compositions in acid, neutral and alkaline solutions. A surface enrichment in platinum due to a preferential dissolution of palladium in all the electrolyte media and an increase of the roughness factor with an increase of the palladium content were observed. In alkaline solution, the exchange current densities for the MOR presented a pronounced maximum for a surface composition of about 15 at% in palladium. This synergistic effect is important, since the exchange current densities are up to 10 times greater than for platinum. Conversely, in acid and neutral media, there is no such maximum and the exchange current densities decrease monotonically from pure platinum to pure palladium. This enhanced MOR electroactivity in alkaline media at the Pt-Pd catalyst was explained on the basis of a decrease of electrode poisoning.

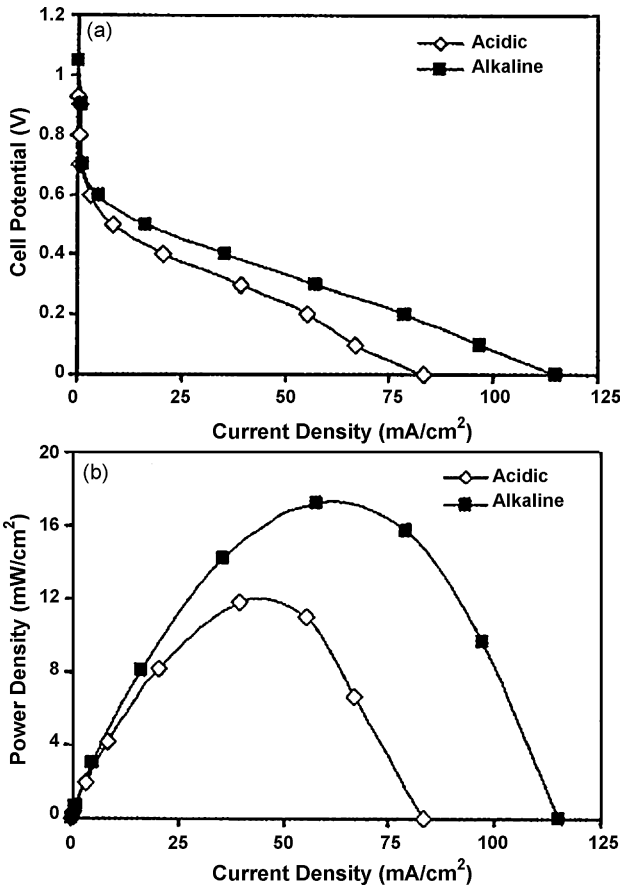

Fig. 1. Polarization and power density curves for an air-breathing, direct-methanol LFFC operated in either alkaline or acidic media at room temperature.
Reprinted from ref. [31], copyright 2006, with permission from The Electrochemical Society.

Gold is recognized to adsorb oxygen containing species in alkaline solution at a more negative potential than in acidic solution, so, based on the bi-functional theory of electrocatalysis, the presence of gold atoms is expected to enhance the electrocatalytic activity of platinum electrode for methanol oxidation in alkaline solution but not in acidic solution [33]. Watanabe and Motoo [33] observed the activity maximum for the MOR on Pt–Au alloys at 40 at% Au. The activity was enhanced about 2.5 times compared with that of Pt in alkaline solution. On the contrary, no enhancement was exhibited in acidic solution by alloying. More recently, nanosized gold has been reported to have the excellent catalytic activity for CO oxidation [34,35], thus it could be suitable to decrease the poisoning effect of CO_{ads} at the Pt-based catalyst surface. So, the co-catalytic effect of gold for methanol electro-oxidation at Pt-based catalysts has attracted many attentions [36–38]. Luo et al. [36] investigated the MOR activities in alkaline electrolytes of Au-Pt/C catalysts with different composition ranging from 10% to 90% Au. The catalysts with 65–85% Au exhibited maximum electrocatalytic activities. The findings revealed important insights into the participation of CO_{ads} and OH_{ads} on Au sites in the catalytic reaction of Pt in the Au–Pt alloys with 75% Au.

Noble (Au) [33] and non-noble (Cd,Pb,Bi,Tl) [23] metal ad-atoms were investigated as MOR promoters on Pt in alkaline media. When these metals are present in alkaline solutions at low concentrations, methanol oxidation on Pt electrodes is enhanced in the low potential range of interest for fuel cell anodes. At higher concentrations of these species, methanol oxidation is suppressed due to excessive coverage by foreign metal ad-atoms. The ad-electrode Au-Pt presented the same electrocatalytic characteristics for methanol oxidation as the Au–Pt alloy electrode. This finding indicates the surface composition to play predominant roles in the methanol oxidation [33].

Recently, some metal oxides (CeO_2, NiO, V_2O_5) [39–42] have been tested as promoters for the MOR in alkaline media on Pt. Oxide promoted Pt showed higher MOR activity than Pt alone. The higher activity and better poison resistance of the Pt-M_xO_y catalysts was attributed to the synergistic effect between Pt and oxide promoter.

Perovskites were also investigated as promoters of the MOR on Pt. The perovskite-modified ($La_{1-x}Sr_xCoO_3$ and $La_{1-x}Sr_xMnO_3$) Pt/C electrodes were more active than the Pt/C electrode for methanol electro-oxidation in alkaline solution. The higher electrocatalytic activities of the perovskite-modified Pt/C compared with Pt/C alone was ascribed to the advantageous role of the perovskite oxides in promoting the formation of the active platinum oxides/hydroxides, providing oxy-species at a less positive potentials [43].

2.1.2. Pt-free catalysts

Among different metals, nickel is the most investigated Pt-alternative anode catalysts for methanol oxidation in alkaline media. Since nickel placed in contact with a solution of aqueous alkali has been shown to become covered with a layer of nickel hydroxide, the surface change is normally written as:

$$Ni(OH)_2 \rightarrow NiOOH + H^+ + e^- \quad (1)$$

although it is recognised that the oxidation state of the nickel in the oxide layer probably changes continuously between two and four over a range of potentials [44]. The oxidation of primary alcohols at Ni/NiOOH electrodes in alkaline medium leads to the formation of organic acids [44]:

$$RCH_2OH + NiOOH \rightarrow RCOOH + Ni(OH)_2 \quad (2)$$

A general mechanism of the oxidation of primary alcohols at Ni/NiOOH electrodes in alkaline medium was proposed by Fleischmann et al. [44]. Kowal et al. [45] investigated the electrochemical oxidation of methanol at Ni hydroxide electrodes in alkaline electrolytes. They found that methanol oxidation commences in the potential region where multi-layers of NiOOH are formed on the electrode surface, and occurs in two stages, with predominantly formate being formed in the potential window 0.36–0.44 V (vs. SCE), followed by further oxidation to carbonate at potentials above approx. 0.45 V. Rahim et al. [46] observed that the reaction of the electro-oxidation of methanol in alkaline medium on Ni dispersed on graphite electrodes is activation controlled proceeding by direct chemical reaction with NiOOH for thin nickel oxides and by charge transfer with the electrode for thick oxides. Recently, a novel titanium-supported nano-scale nickel catalyst (nanoNi/Ti) with flaky structures was prepared by Yi et al. [47]. Cyclic voltammograms in alkaline solutions showed that the oxidation current of methanol on the nanoNi/Ti was much higher than that on a polycrystalline nickel. Chronoamperometric measurements indicated that the steady-state current on the nanoNi/Ti was significantly higher than on conventional Ni and linearly proportional to the methanol concentration. The results showed that this novel nickel electrode can be used repeatedly and possess stable electrocatalytic activity for the methanol oxidation.

In addition to the pure nickel electrode, different nickel-based electrodes, like nickel alloy and nickel complex modified carbon electrodes, have been tested for methanol oxidation in alkaline media. The MOR activity of Ni can be enhanced by alloying with Ru and Cu. Kasakov et al. [48] observed that the electrocatalytic activity of Ni–Ru alloys for methanol oxidation in alkaline solutions is higher than that of Ni and Ru alone and rises with the Ru content increasing to 80%. Gobal et al. [49,50] investigated the redox

process and electrocatalytic activities towards the MOR in alkaline media of nickel and nickel–copper alloy modified glassy carbon electrodes. The addition of copper to the electrodeposited nickel is a very effective method of suppressing the formation of γ-NiOOH species, less effective for the MOR than β-NiOOH species, during prolonged cycling processes in alkaline medium. The methanol electro-oxidation at the Ni–Cu alloy (40% Cu) modified electrode was significantly larger than that at pure Ni.

Research into developing new electrode materials is also directed towards the use of macrocyclic complexes of some metals in the form of conductive polymers. An immobilised polymeric film containing a reversible redox centre acts as a fast electron-transfer mediator for a solution species, which is oxidised or reduced slowly or not at all at the naked electrode. Macrocyclic complexes of nickel are of particular interest as modifying agents because in basic media nickel redox centres show high activity towards the oxidation of some small organic compounds [51,52]. Thus, Ni-complex modified electrode systems have been tested for the MOR in alkaline solutions [52–58]. All these systems showed a MOR activity in NaOH solution higher or comparable to that of bare Ni. One of the main advantages of redox polymers with the coordinated redox couple is the higher chemical stability of the attached redox centre compared with electrostatically incorporated sites. The physical stability of the polymer films is also very often satisfactory, due to the insolubility of the polymers in the aqueous electrolytes.

Palladium and gold are active for methanol oxidation in alkaline media [32,33,59–61], but their activity is remarkably lower than that of platinum [40,62]. The MOR activity of Pd can be enhanced by the presence of a second metal, as in binary Pd-Au [33] and Pd-Ni catalysts (with Ni either alloyed [63,64] or in the oxide form [65]). The MOR activity of Au, instead, can be increased by using specific metal structures, as continuous gold films deposited on the surface of ultrafine PAni fibers [66] or isle-like Au nanoparticle formed on modified ITO electrodes [67].

The perovskite oxides of the general compositions ABO_3 and A_2BO_4 with excellent electrical conductivities and electrocatalysis were considered as possible materials for the application as anode materials in direct methanol fuel cells (DMFCs). White and Sammells [68] observed that perovskite electrocatalysts are active towards methanol oxidation during CV measurements in H_2SO_4. On this basis, perovskite oxides have been investigated as electrocatalysts for methanol oxidation in alkaline media. A series of rare earth cuprates with overall composition $Ln_{2-x}M_xCu_{1-y}M_y'O_{4-\delta}$ (where Ln = La and Nd; M = Sr, Ca and Ba; M′ = Ru and Sb: $0.0 \le x \le 0.4$ and $y = 0.1$) were tested as anode electrocatalysts for methanol oxidation in alkaline media by Raghuveer et al. [69]. These materials showed significant activity for the MOR at higher potentials. The linear correlation between Cu^{3+} content and methanol oxidation activity suggested that the active sites for adsorption of methanol are Cu^{3+} ions. These materials showed better tolerance towards the poisoning by the intermediates of methanol oxidation compared to that of conventional noble metal electrocatalysts. The lattice oxygen in these oxides could be considered as active oxygen to remove CO intermediates of methanol oxidation reaction. The high values of Tafel slopes obtained for rare earth cuprates compared to that of platinum in the methanol adsorption region suggest that the adsorption of methanol is the rate-determining step on these oxides. Yu et al. [70] investigated the electrocatalytic activity of $La_{1-x}Sr_xMO_{3-\delta}$, where M = Co and Cu, towards methanol oxidation in 1 M NaOH. The methanol oxidation onset potential for $La_{1-x}Sr_xCoO_{3-\delta}$, was 0.42 V, 0.03 V lower than that for $La_{1-x}Sr_xCuO_{3-\delta}$. However, the electrocatalytic activity for methanol oxidation of $La_{1-x}Sr_xCuO_{3-\delta}$ was much higher than that of $La_{1-x}Sr_xCoO_{3-\delta}$. The authors ascribed the higher electrocatalytic activity for $La_{1-x}Sr_xCuO_{3-\delta}$ to the capability of Cu ions for the absorption of methanol and the existence of a large amount of oxygen vacancies facilitating oxygen ion (O^{2-}) transport into the proximity of adsorbed methanol oxidation intermediates at the reaction site.

Singh et al. [71] studied the MOR activity in an alkaline solution at 25 °C of $La_{2-x}Sr_xNiO_4$ ($x = 0$, 0.25, 0.5 and 1.0). The results showed that all the $La_{2-x}Sr_xNiO_4$ are quite active for the MOR in alkaline medium and the electrocatalytic activity increases with x. All the perovskites investigated did not indicate any poisoning by the methanol oxidation intermediates/products. The MOR activity of $La_{2-x}Sr_xNiO_4$ was compared with that of pure Pt. The onset potential for electro-oxidation of methanol on Pt was significantly lower than that on $La_{2-x}Sr_xNiO_4$, however, the observed apparent current densities are considerably low at Pt compared to that on $La_{2-x}Sr_xNiO_4$. The observed low oxidation current densities on Pt can be caused to the poisoning of the direct methanol fuel cells electrode surface by the oxidation intermediates. To improve the electrocatalytic activities of $La_{2-x}Sr_xNiO_4$ catalysts, the electrodes were modified by finely dispersed nickel particles [72]. The results showed that the apparent electrocatalytic activities of the modified oxide electrodes are much higher than those of unmodified electrodes under similar experimental conditions. The highest activity was obtained with the Ni-modified $La_{1.5}Sr_{0.5}NiO_4$ electrode. At 0.55 V (vs. Hg|HgO) in 1 M KOH/1 M CH_3OH at 25 °C, this electrode delivered a current density of over 200 mA cm^{-2}. According to the authors, such high methanol oxidation current densities have not been reported on any other non-platinum electrode in alkaline solution.

2.2. Catalysts for ethanol oxidation in alkaline media

Among pure metals, palladium is the more active catalyst for the ethanol oxidation reaction (EOR) in alkaline media. Conversely to ethanol oxidation in acid media, in alkaline media the EOR activity of Pd is remarkably higher than that of Pt [39]. Xu et al. [73] compared the EOR activity in alkaline medium of Pt and Pd supported on carbon Vulcan and carbon microspheres (CMS) by cyclic voltammetry. The onset potential for ethanol oxidation on Pd shifted at lower potentials with respect to that on Pt. The current density peak on Pd was higher than on Pt. These results indicate that the activity for ethanol oxidation is higher on Pd than on Pt, independently of the type of support, also if the difference is more significant for the catalysts supported on CMSs. Liang et al. [74] studied the mechanism of the EOR on Pd by CV measurements. They found that acetate is the final product and acetaldehyde is an active intermediate. The content of the carbonate ions in the solution indicated that less than 5% of the ethanol was converted to the carbonate ions. This result indicates that, as in the case of ethanol oxidation in acid medium on Pt [16], the cleavage of the C–C bond is rather difficult on the Pd catalyst and acetate ions are the main product of the EOR. They also found that the dissociative adsorption of ethanol proceeds rather quickly and the rate-determining step is the removal of the adsorbed ethoxy by the adsorbed hydroxyl.

As nanowire arrays have attracted more interest due to their excellently physical and chemical properties, highly ordered Pd nanowire arrays, prepared by a template-electrodeposition method, were investigated as catalysts for ethanol oxidation in alkaline media [75]. The activity of Pd nanowire arrays for ethanol oxidation was not only higher than that of Pd film, but also higher than that of a commercial Pt-Ru/C. This nanowire array structure has high electrochemical active surface and permits liquid alcohol to diffuse into the catalyst layer easily, resulting in the reduction of liquid sealing effect.

To improve the electrocatalytic activity of platinum and palladium, the ethanol oxidation on different metal ad-atom-modified, alloyed and oxide promoted Pt- and Pd-based electrocatalysts

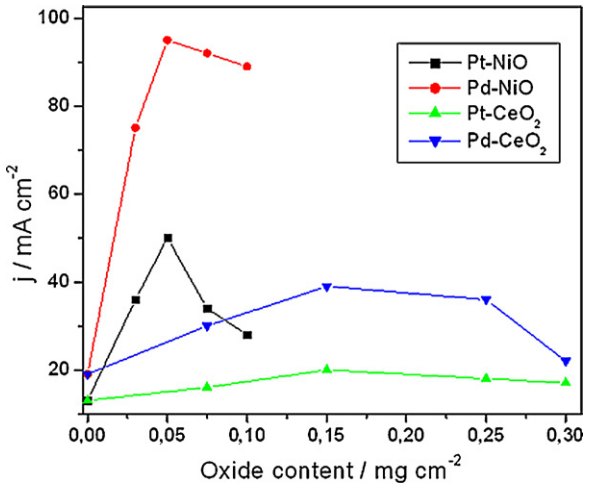

Fig. 2. Effect of the content of oxide in Pt/C and Pd/C catalysts for ethanol electrooxidation in 1.0 M KOH solution containing 1.0 M ethanol with a sweep rate of 50 mV s^{-1}, Pt or Pd loading: 0.3 mg cm^{-2}.
Reproduced from ref. [85], copyright 2007, with permission from Elsevier.

has been investigated in alkaline media. Firstly, El-Shafei et al. [76] studied the electrocatalytic effect of some metal ad-atoms (Pb,Tl,Cd) on ethanol oxidation at a Pt electrode in alkaline medium. All three metal ad-atoms, particularly Pb and Tl, improved the EOR activity of Pt. More recently, bimetallic Pd-M (M = Ru, Au, Sn and Cu) catalysts [77–79] have been tested for ethanol oxidation in alkaline media. Chen et al. [77] found that the catalytic activity of Pd-Ru is considerably higher than that of Pd toward the oxidation of methanol, ethanol, and ethylene glycol. The activity sequence of Pd-Ru toward the alcohol oxidation was ethanol > ethylene glycol > methanol, and Pd-Ru with 1:1 atomic ratio exhibited the highest activity. They also compared the activities of Pd-Ru and Pt-Ru catalysts for alcohol oxidations in alkaline media. For the oxidation of methanol and ethylene glycol, the activity of Pd-Ru was lower than that of Pt-Ru. For ethanol oxidation, instead, the activity of Pd-Ru was higher than that of Pt-Ru. At potentials ranging from 0.3 to 0.4 V, the mass specific activity of Pd-Ru was almost 4 times that on Pt-Ru. He et al. [78] prepared Pd_4Au/C and $Pd_{2.5}Sn/C$ catalysts and compared their EOR activity with that of a commercial Pt/C. The results indicated that, although Pt/C showed better kinetics for ethanol oxidation, as manifested by the more negative onset potential and larger instantaneous current density, Pd_4Au/C and $Pd_{2.5}Sn/C$ were more tolerant to poisoning. Among the catalysts investigated, Pd_4Au/C displayed the best EOR activity in alkaline media. Jou et al. [79] compared the EOR activity in an alkaline solution of a Pd-Cu-coated ITO electrode (Pd:Cu 90:10) with that of a Pd-coated ITO electrode. The onset potential for ethanol oxidation on the Pd-Cu-coated electrode was 150 mV more negative than that observed on the Pd-coated electrode. The results indicated that the Pd-Cu alloy electrode has higher EOR activity and better capability against poisoning than Pd.

The effect of addition of various oxides to carbon supported Pt and Pd catalysts on ethanol oxidation in alkaline media was investigated [80–87]. The addition of oxides such as CeO_2 [80,83,85,86], ZrO_2 [81], MgO [82], Co_3O_4 [83,86], Mn_3O_4 [83,86], NiO [83–86] and In_2O_3 [87] remarkably improved the EOR activities of Pt/C and, in particular, Pd/C and moved the onset potentials towards lower values. The effect of the content of oxide in Pt/C and Pd/C catalysts on the EOR activity is shown in Fig. 2 from ref. [85]. The electrocatalysts with the weight ratio of Pt or Pd to CeO_2 of 2:1 and Pt or Pd to NiO of 6:1 showed the highest electrochemical catalytic activity for ethanol oxidation. According to Xu et al. [82], it is possible that oxide functions as Ru does in Pt-oxide and Pd-oxide catalysts because OH_{ad} species could easier form on the surface of oxide. The formation of OH_{ad} species at lower potential can transform CO-like poisoning species on the surface of noble metal to CO_2 or other products. In particular, among various oxide promoted Pd catalysts, Pd-NiO showed the highest EOR activity, with the lowest onset potential and the highest peak current density [83].

Spontaneous deposition of noble metals onto less-noble metal particles or metal surfaces is an alternative method to electroless and electrodeposition techniques for manufacturing electroactive materials [88]. Recently, it was discovered that Raney nickel materials can be successfully employed as supports for noble-metal catalysts to give effective anodes in aqueous ammonia electrolyzers [89]. On theses bases, Bambagioni et al. [90] prepared Pd-based catalysts by the spontaneous deposition of Pd on Ni–Zn and Ni–Zn–P alloys supported on carbon. An advantage of Ni-Zn materials as substrates for spontaneous deposition procedures is just the presence of Zn, which is more electropositive than Ni and therefore prone to undergo transmetalation with Pd^{II} or Pd^{IV}. The analytical and spectroscopic data showed that the surface of Pd-(Ni-Zn)/C and Pd-(Ni-Zn-P)/C contain very small (0.5–1 nm), highly dispersed, and crystalline palladium clusters as well as single palladium sites, likely stabilized by interaction with oxygen atoms from Ni-O moieties. The ethanol oxidation reaction on Pd-(Ni-Zn)/C and Pd-(Ni-Zn-P)/C was compared with that of a conventional carbon supported Pd. The results obtained in the half cell indicated that the EOR activity of Pd-(Ni-Zn)/C and Pd-(Ni-Zn-P)/C is only slightly superior to that of Pd/C, but the chronopotentiometric tests showed lower overpotentials on Pd-(Ni-Zn)/C and Pd-(Ni-Zn-P)/C electrodes.

A new group of Ru-Ni and Ru-Ni-Co catalysts for ethanol oxidation in alkaline media was investigated by Kim and Park [91,92]. The electro-oxidation of ethanol on thermally prepared ruthenium oxide in alkaline solution was firstly investigated by Hsieh et al. [93]. The redox couple of ruthenate (Ru(VI)) and perruthenate (Ru(VII)) on the RuO_2 electrode surface was observed during the oxidation of ethanol. As previously reported, a redox couple of nickel, i.e., nickel hydroxide ($Ni(OH)_2$) and nickel oxyhydroxide (NiOOH), was shown to be involved in the oxidation of alcohols at nickel electrodes in alkaline media [44]. On this basis, the RuO_2 system on the Ni support is expected to possess high electrocatalytic activity during oxidation of organic compounds. As reported by Kim and Park [91], the RuO_2-Ni electrode showed higher activity for ethanol oxidation in 1 M NaOH than the Ni electrode. The net anodic peak current densities for ethanol oxidation at the RuO_2-Ni electrode were 6.3 and 1.7 times larger than those observed at the Ni electrode, in 0.1 and 0.5 M ethanol, respectively. A synergistic effect between Ru and Ni oxides was proposed. Electrochemical deposition is the most common method of making nickel hydroxide electrodes. Commonly, nickel hydroxide is precipitated from a solution of nickel nitrate and sodium nitrate dissolved in an ethanol–water mixture. The sodium nitrate provides excess nitrate to enhance the precipitation, and the presence of the ethanol changes the surface-tension characteristics of the precipitation process, improving adhesion of precipitate to the current collector [94]. For this reason, in a next work, Kim and Park [92] used the sodium nitrate to prepare the base nickel electrode and Ni electrodes with Ru and Co as additives. CVs of these electrodes in alkaline media are shown in Fig. 3. The nickel electrodes containing Ru and/or Co showed higher EOR activity than Ni alone. The ethanol oxidation onset potentials shifted to more negative values and the current densities were higher than pure Ni. The Ni-Co-Ru electrode, with an anodic peak potential more negative than that of nickel by about 70 mV, and an anodic current density of about 1.4 times higher than that of Ni electrode showed the best electrochemical characteristics. Addition of cobalt lowers the oxidation

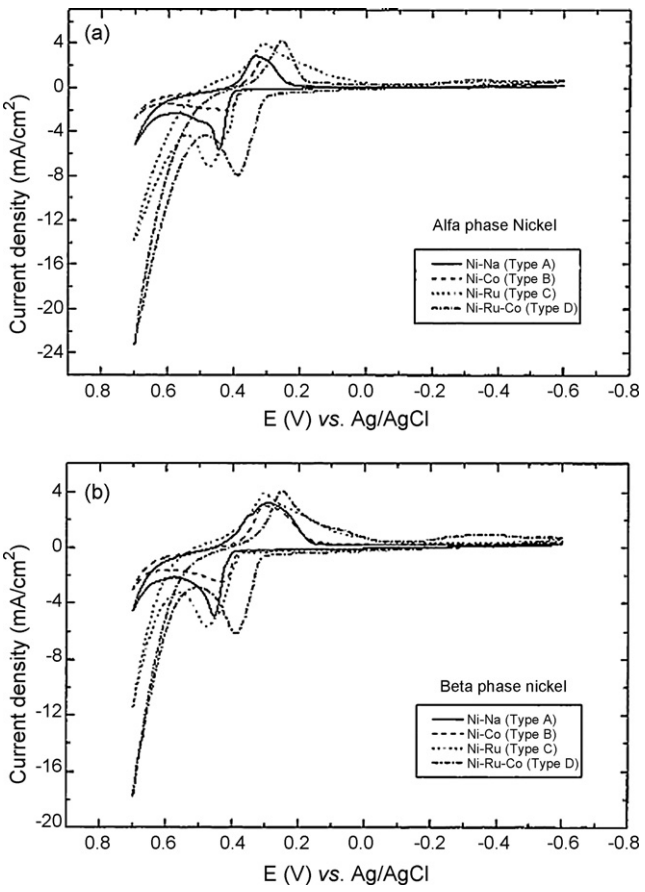

Fig. 3. CVs of various electrodes electrochemically prepared (a) α-phase and (b) β-phase nickel electrodes in 1.0 M KOH at a scan rate of 5 mV s^{-1}.
Reprinted from ref. [92], copyright 2003, with permission from The Electrochemical Society.

potential, while ruthenium increases the current density for the anodic process and shifts the oxygen evolution potential to a more negative value. When both ruthenium and cobalt are used as additives, the redox potential shifts to an even more negative value than that for Ni with Co and Na. XANES data for the Ni and Co K-edges of these composite electrodes revealed that both Ni and Co are in the Ni^{3+}-Ni^{4+} and Co^{3+}-Co^{4+} mixed states, respectively, depending on applied potentials.

An Italian company, Acta, has recently reported good activity for the EOR, with complete oxidation to CO_2 or carbonate, on anodes consisting of small nanoparticles or clusters of Ni–Fe–Co alloys in a matrix of hydrazone-based polymer, with the trade name HYPERMEC™ [22].

2.3. Catalysts for ethylene glycol oxidation in alkaline media

Ethylene glycol (EG) is of particular importance as an energy carrier for fuel cells because of its high energy densities, ease of transport, favourable storage, low vapour pressure, non-toxic nature and ready availability. Starting from the middle of 1970s, the anodic oxidation of ethylene glycol in alkaline media has been extensively investigated both from an electrocatalytic point of view and for its possible use in fuel cells. The overall oxidation reaction, which needs up to 10 electrons per molecule when the final state of oxidation (i.e. CO_2) is reached, proceeds through several consecutive and parallel steps, involving different reaction intermediates. Platinum is commonly used as catalyst for EG oxidation, also if gold presents higher current densities than Pt [95]. Chang et al. [96] studied the electrooxidation pathways of ethylene glycol in alkaline aqueous solution on gold and platinum. The electrooxidation on gold featured the successive formation of partially oxidized C_2 solution species en route to oxalate and carbonate production. The latter species was produced predominantly via the formation of the dialdehyde, glyoxal. In contrast, ethylene glycol electrooxidation on platinum exhibited markedly different kinetics and product distributions to those for the partially oxidized C_2 species, inferring that at least carbonate production from ethylene glycol occurred largely through sequences of chemisorbed, rather than solution-phase, intermediates. Hahn et al. [97] investigated the adsorption of ethylene glycol at a platinum electrode in aqueous medium. The adsorption appeared to be dissociative at any pH. However, striking changes occurred in the composition of the adsorbed layer when the pH varied from acid to alkaline solutions. Linearly bonded CO was dominant at pH ∼ 1, whereas almost equal amounts of bridge-bonded and linearly bonded CO species were found at pH ∼ 13. Christensen and Hamnett [98] investigated the electro-oxidation of ethylene glycol at Pt electrodes in acidic and basic solutions by in situ FTIR spectroscopy. In acid, the main products were glycolic acid and CO_2, and the reaction is shown to proceed through a relatively small number of reactive sites. These active sites were poisoned at intermediate potentials, and the poisoning species were identified as terminally bonded CO. In alkali, the main products are glycolate, oxalate and CO_3^{2-}. Production of glycolate and carbonate appeared to take place via the same intermediate, but oxalate was apparently produced by further oxidation of desorbed glycolate. Poisoning also took place in alkali medium. Matsuoka et al. [99] investigated the electrochemical oxidation of ethylene glycol at 400 and 500 mV on platinum in alkaline solution. By analyzing the oxidation products they concluded that there were two paths for ethylene glycol oxidation: poisoning and non-poisoning paths. The poisoning path led to the production of C_1 compounds and the non-poisoning path gave oxalate. Most of the C–C bond cleavage in ethylene glycol could not take place below 400 mV, which would prevent CO poisoning of platinum. On the other hand, the C–C bond of ethylene glycol was cleaved in ethylene glycol oxidation at 500 mV, which led to CO poisoning.

The electrocatalytic activity of platinum for the ethylene glycol oxidation reaction (EGOR) can be improved using binary systems obtained either by alloying platinum with different metals, or by modifying a platinum surface by foreign metal ad-atoms. Kohlmuller [100] observed that the intermetallic compound Pt_3Pb exhibited an activity approximately ten times higher than pure platinum in the anodic oxidation of ethylene glycol to oxalic acid in 6 M KOH. Dalbay and Kadirgan [101] investigated the electrocatalytic oxidation of ethylene glycol on Pt, Pd and Pt–Pd alloy electrodes of different compositions in alkaline solution. The exchange current density of Pt–Pd alloys went through a maximum at about 20 at% Pd, greater than those for pure metals, so indicating a synergistic effect. This effect was ascribed to a decrease of strongly bound residue of ethylene glycol. Kadirgan et al. [102] investigated seven different foreign metal ad-atoms (Bi,Cd, Cu,Pb,Re,Ru,T1) as activity modifiers of a platinum electrode for the EGOR in alkaline medium. All these metal ad-atoms increased the electrocatalytic activity of the Pt electrode for the optimum foreign metal concentrations in solution. This enhanced activity, which can reach very high values, close to diffusion-limited current densities with the best foreign metals (Pb and Bi), was explained through the bifunctional theory of electrocatalysis. Conversely, in acid medium the presence of the same ad-atoms does not enhance the electrocatalytic activity of Pt. El-Shafei et al. [103] studied the electrochemical oxidation of ethylene glycol on Pt, Pd and Au electrodes in alkaline medium in the absence and in the presence of metal ad-atoms. For pure-metal electrodes, the maximum current density was obtained

at the Au electrode. However, in the presence of metal ad-atoms, enhancement of catalytic activity changed its order to: Pt > Au > Pd. The three different electrodes showed maximum catalytic activity when modified with Pb ad-atoms. More recently, Demarconnay et al. [104] observed that the addition of Bi to platinum leads to decrease the onset potential of EG electrooxidation of about 70 mV and to achieve higher current densities. The ternary catalyst Pt-Pd-Bi/C does not change the onset potential of EG oxidation, but leads to increase the current densities compared to Pt-Bi/C. They found that the addition of foreign atoms to platinum led to decrease the ability of the catalyst to break the C–C bond, likely due to dilution of surface platinum atoms. But, in the same time, catalyst containing Pd and Bi seems to activate the oxidation of EG to oxalate compared to pure platinum. They proposed that Bi mainly favors the adsorption of OH species but also affects the product distribution by changing the composition of chemisorbed species, whereas Pd only limits the poisoning of Pt sites by changing the composition of chemisorbed species.

It was demonstrated that gold is a very good catalyst for the electrochemical oxidation of aldehydes and alcohols in alkaline solutions [95]. However, the potentials at which the maximum current densities occur are too positive for practical applications in fuel cells. These difficulties may be overcome using gold platinum alloys, as reported by Beden et al. [105]. They carried out the oxidation of ethylene glyco1 on a Pt-Au electrode (48.4 at% Au surface composition) by CV. During the positive sweep, the EG oxidation occurs in two main peaks, the first one at 0.76 V/RHE, in the same potential range as that for EG oxidation on pure Pt, and the second one at 1.18 V/RHE, corresponding to oxidation on pure Au. However, the current densities obtained with Pt–Au alloy electrodes were much higher than those on pure metals, particularly in the Pt region of the alloy, since the current density for this alloy was about eight times greater. The catalytic activity of the Au region of the alloy was also enhanced, but only by a factor of two. This high activity was ascribed to synergistic effects between Pt and Au. They also observed that underpotential deposition of Pb ad-atoms on a Pt–Au alloy electrode greatly enhances the EGOR activity in alkaline medium of this alloy. The synergistic effect between Pt and Au was observed also by El-Shafei et al. [106]. They studied the EGOR at Pt, Au and Pt-Au alloy deposited electrochemically on a glassy carbon (GC) substrate. Pt-Au/GC showed higher activity compared with that of Pt/GC and Au/GC. The current density obtained on Pt-Au/GC electrodes in the Pt region was much higher than that on the Pt/GC electrode, resulting in a catalytic factor of about 5 at the optimum alloy composition (40 at% Pt). More recently, Jin et al. [107] investigated the EGOR on platinum-gold catalysts by CV. They observed the presence of a large oxidation peak in the potential range of pure platinum and a second small peak in the potential range of pure gold. Given that similar peak current densities have been reported for Pt and Au electrodes [108] and that the Pt-Au nanoparticles were prepared with a 1:1 atomic ratio, a synergistic effect of Au presence on the Pt activity, but not of Pt presence on Au activity for EG oxidation can be inferred. Gold has higher electronegativity than platinum, so the interaction between platinum and gold in the Pt-Au nanoparticles may change the distribution of electrons in platinum, making the adsorption of ethylene glycol and hydroxyl on platinum easier. Summarizing, both Au and Pt are good electrocatalysts for EG oxidation, but in Pt–Au alloys gold overall acts as promoter of the EGOR on Pt.

Kadirgan et al. [109] investigated the electrochemical oxidation of ethylene glycol on gold and ad-atom-modified gold electrodes in alkaline medium. As in the case of Pt, the influence of different metal adatoms (Bi,Cd,Cu,Pb,Re,Ru,Tl) on the catalytic properties of Au electrodes was considered. In contrast to the case in acid medium, the spectroscopic results showed clearly that almost no C–C bond scission occurs during adsorption in alkaline medium. Depending on the potential of electrolysis, the major products of the reaction were found to be glycolate alone, or a mixture of glycolate, oxalate, carbonate and formate. Compared to Au alone, only the Au-Bi and Au-Pb electrodes appeared to be relatively interesting. These systems shifted the polarization curves towards more negative potentials, reducing the overvoltage by about 100 mV, but without changing the magnitude of the current density. Recently, Matsuoka et al. [110] deposited ultrafine gold on α-Fe_2O_3/Pt/C electrodes. Compared to Pt/C catalyst for ethylene glycol oxidation, the Au/α-Fe_2O_3/Pt/C electrode showed higher catalytic activity for the oxidation of ethylene glycol in alkaline solution in the potential range lower than 500 mV.

3. Cathode catalysts

3.1. Oxygen reduction in alkaline media

Generally, the kinetics of the oxygen reduction reaction (ORR) is more facile in alkaline medium than in acid medium [3,4]. Blizanac et al. [4] used a thermodynamic analysis to explain the origin of the pH effect, showing that the overpotential required to facilitate the 4-electron transfer process at high pH is relatively small compare to the potential required at low pH in the case of Ag(1 1 1). At high pH, no specific chemical interaction between the catalyst and O_2 or O_2^- is required, whereas strong chemical interaction is necessary at low pH.

Oxygen reduction in aqueous alkaline media is a complicated electrocatalytic reaction. The ORR is a complex process involving four coupled proton and electron transfer steps. Several of the elementary steps involve reaction intermediates leading to a wide choice of reaction pathways. According to Spendelow and Wieckowski [22], the various pathways of the ORR can be divided into three groups. Two of these lead to OH^- as the final product (complete reduction, with transfer of four electrons), and one leads to peroxide (partial reduction, with transfer of two electrons). The four-electron pathways are often described as the direct pathway and the series pathway, the difference being that the former proceeds directly to OH^-, while the latter produces hydrogen peroxide (existing as HO_2^- in alkaline media) as an intermediate which is subsequently further reduced to OH^-.

The low activity of catalysts in acid media is exacerbated by the presence of spectator species adsorbed onto the electrode surface, which act to physically block the active sites and also lower the adsorption energy for intermediates, so retarding the reaction rate [4]. Since adsorption of spectator ions inhibits many electrocatalytic processes, the decreased extent of anion adsorption in alkaline media means that, in general, most electrocatalytic processes should be more facile in alkaline solutions than in acidic solutions.

Due to the inherently faster kinetics for the ORR in alkaline media, a wide range of supported and unsupported catalysts have been studied including noble metals, non-noble metals, perovskites, spinels, etc. In alkaline media the carbon support plays a role in the kinetics as well as the catalyst supported on its surface, so the performance of the catalyst/support system has to be considered since carbon participates in the reaction by a 2-electron process.

While the electrocatalytic advantages of using alkaline media are significant, the improved material stability afforded by the use of alkaline electrolytes is even more important. Very few electrode materials are stable under strongly acidic conditions, especially under the strongly oxidizing conditions encountered at oxygen cathodes. In contrast, a much wider range of materials are stable in alkaline environments, including much less expensive materials such as Ni and Ag.

3.2. Catalysts for oxygen reduction in alkaline media in the absence of alcohol

In ADAFCs the alcohol crossover is reduced by (1) the way of ion transport within the membrane, occurring in the direction opposite to, and hence reducing the level of, fuel crossover through the membrane, and (2) the use of membranes with low alcohol permeability. On these bases, generally, it is possible to use in ADAFCs the same cathode catalysts used in H_2/O_2 AFC. Excellent reviews on cathode catalysts for oxygen reduction in alkaline media in the absence of alcohol have been done by Spendelow and Wieckowski [22] and by Bidault et al. [13]. Thus, the catalysts for the ORR in alkaline media in the absence of alcohol will be only briefly treated in the following paragraph.

3.2.1. Noble metal catalysts

Among pure metals, platinum is the more active catalyst for the electro-reduction of oxygen in alkaline media. Experimental studies in alkaline media indicated that four-electron ORR predominates on Pt cathodes [111], though even in the case of the four-electron process the reaction proceeds at least in part via a HO_2^- intermediate (the series pathway) [112]. Carbon-supported Pt is commonly used as cathode catalyst in low-temperature fuel cells. Two features affect the use of carbon as catalyst support in alkaline media, i.e. its thermal stability and its ORR activity. The corrosion of the carbon cathode support can limit durability. The highest temperature at which carbon shows suitable long-term stability at high potential in strong alkali has been estimated as 75 °C [22]. On the other hand, whereas carbon supports are not electrochemically active in acidic media, carbon blacks and graphite possess catalytic activity for the ORR in alkaline media with the formation of HO_2^- in a two electron process. The resulting increased hydrogen peroxide production by oxygen reduction on carbon could lead to elevated rates of degradation of fuel cell components. However, Genies et al. [113] found that O_2 reduction currents on carbon are negligibly small compared to currents on supported platinum particles.

The oxygen reduction was investigated in alkaline media on different Pt-based alloys: generally Pt–M alloys, with M = Pd [114], Ta [115], Co [116,117], Au [118], V [119] and Pb [120], showed higher activity than Pt. The improvement in the ORR activity of Pt-alloys was explained by geometric (change in Pt–Pt bond distance) and electronic (changes in the Pt 5d electronic density) effects and by the presence of surface oxides. The ORR activity of Pt–Ag alloys, instead, was lower than that of Pt [121].

The effect of Pd modification of Pt surfaces on the ORR activity in alkaline electrolyte was studied by Schmidt et al. [122]. They found that the kinetics of the ORR is significantly enhanced by modification of Pt(*h k l*) surfaces with Pd. Even on the highly active Pt(1 1 1) surface the kinetics can be improved by a factor of approximately two to four due to Pd modification. Lima et al. [123] studied the kinetics of the ORR in an alkaline electrolyte on well-ordered single-crystal surfaces of Au(1 1 1), Ag(1 1 1), Pd(1 1 1), Rh(1 1 1), Ir(1 1 1), and Ru(0 0 0 1) and on nanoparticles of these metals dispersed on Vulcan carbon. Plots of the kinetic currents of the ORR on these types of electrode surfaces showed a volcano-type dependency on the d-band center of the metal catalyst. Pd showed particularly high activity, suggesting it may offer potential replacement for Pt in fuel cells. Some works have been addressed to the ORR on Pd catalysts in an alkaline media [62,123–126]. Yang et al. [124] observed that a finely dispersed Pd/C catalyst has high catalytic activity both for oxygen and for HO_2^- reduction in alkaline solution. Jiang et al. [125] compared the ORR activity in alkaline solutions of Pd/C and Pt/C catalysts. The exchanged electron number per oxygen molecule for the ORR was 4 on both the Pt/C and the Pd/C. The ORR was more favorable on a clean Pd surface than on a clean Pt surface; however, Pd was more easily oxidized at fuel cell cathode working potentials. Bunazawa and Yamazaki [62] found that the ORR activity in alkaline media of Pd/C and Pd-Au/C catalysts, prepared by means of ultrasonic synthesis, was comparable to that of a commercial Pt/C. Kim et al. [126] prepared Pd/C and Pd-Sn/C (Pd/Sn atomic ratio 2.5 and 1.7) catalysts under ultrasonic irradiation, and their ORR activity was evaluated in alkaline solution. The Pd-Sn/C catalysts showed a higher ORR activity than that of the Pd/C catalyst. In addition, the Pd-Sn/C catalysts showed a lower Tafel slope and a larger number of electrons transferred than those of the Pd/C catalyst. These results indicate that Sn influences both the kinetics and the mechanism of the ORR.

Silver has been studied as a potential replacement of Pt as an alkaline ORR cathode material due to its reasonably high activity and its lower cost. Moreover, Ag cathodes have been reported to be more stable than Pt cathodes during long-term operation. [127,128]. The ORR activity of Pt, however, is at least 10 times higher than that of Ag catalyst [129]. Silver in alkaline solutions is oxidized in two steps: first a layer of Ag_2O is formed, which is partly oxidized in the second step to AgO [130]. ORR occurs with the participation of 2 and 4-electron processes, depending on the surface state and in particular on its oxidation state and electrode potential [119,121,129,131]. It is important to denote that the effect of increasing electrolyte concentration to high pH levels is positive for silver catalyst but not for Pt catalyst, which is slightly hindered due to greater absorbed species coverage [131]. Silver becomes competitive to Pt due to favored kinetics in high concentration alkaline media.

The effect of alloying on the ORR activity of Ag in alkaline media was investigated. Generally, the ORR activity of Ag-M alloys in the optimum Ag:M atomic ratio, with M = Pt [119,121], Co [132], Mg [133] and Sb [134], was higher than that of Ag, but lower than that of Pt.

3.2.2. Non-noble metal catalyst

Noble metals play a key role as catalysts for the ORR in fuel cells. While they offer the advantages of high catalytic activity, high electronic conductivity and good stability, their high costs are a major concern for commercial applications. Considering that the kinetics of oxygen reduction in an alkaline solution are superior than those in acidic media, non-noble metal catalysts can be used in alkaline fuel cells.

Manganese oxides have attracted more attention as potential catalysts for fuel cells [135] because of their attractive cost and good ORR activity. Brenet [136] surveyed the electrochemical reactivity of some mixed oxides, and proposed that the electrochemical reduction of O_2 occurs through reduction and oxidation of the redox couple Mn^{4+}/Mn^{3+}. Matsuki and Kamada [137] observed much higher ORR activity of γ-MnOOH compared with that of γ-MnO_2. Among the numerous varieties of manganese oxides, MnOOH showed the highest ORR activity [138]. For manganese oxides as well as for platinum and silver, it is now well admitted that the four-electron O_2 reduction into OH^- can compete with the 2-electron pathway yielding HO_2^- species. Lima et al. [139] observed lower ORR activity on the MnO_x/C species compared to that on Pt/C. Formation of HO_2^- involving $2e^-$ per O_2 molecule was the main path of the ORR in MnO_x/C catalysts but, at low overpotentials the number of electrons is raised to 4 due to the occurrence of a HO_2^- disproportionation reaction. Roche et al. [140] found that doping MnO_x/C nanoparticles with nickel or magnesium divalent cations can considerably improve their ORR activity. As a result, the M-MnO_x/C (M = Ni,Mg) electrocatalysts showed ORR activities close to 10 wt% Pt/C from E-TEK. Recently, Fukuda et al. [141] presented a one-step through-mask electrodeposition process consisting of the first deposition of insulating tetrabutylammonium bromide (Bu_4NBr) crystals and the subsequent formation of con-

ductive layered manganese oxide in the interstitial spaces of the Bu_4NBr grains. Dissolution of the Bu_4NBr mask gave a porous structure composed of MnO_x nanosheets. The resulting MnO_x-modified electrode showed a larger catalytic current for the reduction of oxygen in alkaline solution, compared to the bare Pt electrode.

Perovskites (ABO_3) and spinels (AB_2O_4) oxides have been investigated for the ORR in alkaline media with moderate success. The performance of transition metal oxides and mixed transition metal oxides is often limited by their low bulk conductivity and low active surface area [142]. Among them, perovskites are considered the leading candidates because of their reasonable electrical conductivity and corrosion resistance. Substituted perovskites can generally be described by the formula $A_{1-x}A'_xB_{1-y}B'_yO_3$. A wide selection of materials using La and Nd in position A, Sr, Ba, Ca in position A′, and Ni, Co, Mn and Ru in position B have been synthesized and shaped into electrodes [142]. The catalytic activities of perovskite-type oxide are quite dependent of the elements of B and the ratios of A/B [143]. Meadowcroft [144] found that the conductivity of $LaCoO_3$ could be increased by doping A (with Sr) and B (with Ni) positions of the material while maintaining the perovskite structure. Regarding the stability, $La_{0.6}Ca_{0.4}CoO_3$ was found to be stable for at least 1300 h in electrodes operated under the conditions of rechargeable Zn/air cells [145]. In an alkaline electrolyte, $LaCoO_3$ and related compounds showed good ORR activities. [144,146–148].

Spinel transition-metal oxides have been also identified as promising electrocatalysts for the ORR. In these compounds the electrocatalytic properties have been related to the presence of the internal redox couple of the transition metals. As mixed-valence oxides, their cationic distribution is the bridge between solid-state chemistry and the electrocatalytic properties. Transition metals can occupy a tetrahedral coordination and/or an octahedral coordination with the oxygen ions. The distribution of the cationic oxidation states within both coordinations depends greatly on the preparation conditions. Cobaltite ($M_xCo_{3-x}O_4$, with M = Cu [149], Ni [150] and Mn [151,152]) and manganite ($M_xMn_{3-x}O_4$, with M = Ni [153] and Cu [154]) spinel oxides are very attractive because they exhibit interesting activities for the ORR. Particularly, $CuCo_2O_4$ favors a total of $4e^-$ in the oxygen reduction process [149], which is critical to obtain high-power density during cell utilization without significant deleterious corrosion effects due to the presence of peroxide species in the electrolyte solution.

Macrocycles have attracted increasing attention as alternative electrocatalysts for oxygen reduction [155]. The initial activity of these catalysts is good, but performance declines rapidly. Heat treatment of such macrocycles at temperatures of 450–900 °C, however, results in high ORR activity in alkaline solutions with long-term stability [155]. Potential electrocatalysts for O_2 reduction in the H_2/O_2 fuel cells are N_4-chelates of Fe and Co such as tetraphenyl porphyrins (TPP), tetramethoxyphenyl porphyrins (TMPP), phthalocyanines (Pc), tetracarboxylic phthalocyanines (PcTc) and dibenzotetraazaanulenes (TAA), adsorbed on the high-area carbon and heat-treated at high temperatures under an inert atmosphere. The effect of the heat treatment at 850 °C on Co-TMPP was examined with emission Mössbauer spectroscopy using Co-57 enriched Co-TMPP [156]. The spectra indicated the presence of cobalt oxides with no evidence of Co-N_4 centers or any other form of cobalt. The metal-free complex H_2TMPP, given similar thermal treatment on a mineral-free carbon support, does not show catalytic activity beyond that of the carbon support, thus confirming the importance of the transition metal to the catalysis. Kiros et al. [157] studied the ORR in alkaline fuel cells on high surface area carbons catalyzed by pyrolyzed Co-TPP The results indicated that the enhanced ORR has to be attributed to the combined effect of the macrocyclic black and cobalt additive, and that, among many causes of electrode performance deterioration, loss of cobalt seems to be the most important factor. Oxygen reduction in alkaline and acid media was investigated by Goikovic el al. [158] at Fe-TMPP-Cl adsorbed on the Black Pearls (BP) carbon and heat-treated at temperatures from 200 to 1000 °C. They found that the O_2 reduction rate increases with increasing in the heat-treatment temperature of the electrocatalyst, reaching a plateau at $700 \leq T \leq 1000$ °C. The reaction rate was higher in alkaline solution on all electrocatalysts examined. Activities of Fe-TMPP-Cl/BP and Pt/BP electrocatalysts were compared. FeTMPP–Cl/BP heat-treated at $700 \leq T \leq 1000$ °C showed similar activity to Pt/BP in alkaline solution. Metal needs not be incorporated in the macrocycle before pyrolysis to obtain an active electrocatalysts. Thus, Mocchi and Trasatti [159] applied pyrolysis to a mixture of a metal salt and a macrocycle separately. They showed that pyrolyzed Co-TMPP + carbon can be replaced with pyrolyzed $CoCO_3$ + TMPP + carbon. The replacement results in an appreciable increase in the ORR activity in alkaline media for a calcination temperature of 800 °C in inert atmosphere. These results suggest that the structure of the metal macrocycle is not the factor responsible for the electrocatalytic activity of the resulting material. The origin of the ORR activity is the simultaneous presence of metal precursor, active carbon and a source of nitrogen.

3.3. Alcohol-tolerant catalysts for oxygen reduction in alkaline media

Firstly, Holze et al. [160] investigated Fe-TMPP supported on carbon and subsequently heat-treated at 800 °C as active catalysts for oxygen reduction in fuel cells using methanol as a fuel and an alkaline carbonate electrolyte. The pyrolized Fe-TMPP was as active as Pt/C and less sensitive toward the establishment of a mixed potential. Indeed, upon addition of 1 M methanol, the polarisation curve of the chelate-loaded electrode remained unchanged, while the Pt/C-catalysed electrode showed a much poorer performance. In the same way, Goikovic et al. [158] observed that the reaction rate of O_2 reduction on Fe-TMPP was not influenced by the presence of methanol either in acid or alkaline solution, showing that this electrocatalyst is methanol-tolerant.

More recently, notwithstanding the reduced alcohol crossover in comparison to acid fuel cells, many works have been addressed to alcohol-tolerant catalysts for the ADAFC. As previously reported, Ag is of great interest for use as cathode catalyst in AFCs. Demarconnay et al. [129] investigated the ORR activity in presence of methanol on Ag/C and Pt/C catalysts. When comparing the activity of Pt/C and Ag/C catalysts in presence of methanol, it appears that the Pt/C catalyst displays the higher catalytic activity between 0.9 and 0.75 V *vs*. RHE. But, between 0.8 and 0.6 V *vs*. RHE, the Ag/C catalyst is less affected by the presence of methanol than Pt/C. For example, at 0.75 V *vs*. RHE, the loss in oxygen reduction current density induced by the presence of methanol, i.e. the difference between the current density obtained in methanol-containing and in methanol-free O_2-saturated solutions, is only close to 1 mA cm^{-2} for Ag/C, whereas it reaches 3–4 mA cm^{-2} for Pt/C. In the same way, Koscher and Kordesh [161] tested the ORR in the presence of methanol on Pt and Ag catalysts at 80 °C and 9 M KOH. When Pt was used, there was a significant drop of the performance even at low methanol content. In the case of Ag, instead, there was no influence of the methanol on the performance, even at high amounts of methanol. Both tungsten carbide (W_2C) and Ag are active for the ORR in alkaline media but their overpotentials are higher compared to that of Pt-based electrocatalysts. However, the overpotential can be significantly reduced on the Ag–W_2C composite electrocatalyst, showing a synergetic effect to improve the ORR activity [162]. This novel electrocatalyst showed high selectivity towards the electroreduction of oxygen in the alcohol-containing solutions.

As previously reported, Pd presents high ORR activity in alkaline media [62,124–126]. Moreover, Pd has poor activity for methanol oxidation in alkaline media, lower than that of Pt [73]. On these

bases, Pd and Pd-based catalysts have been tested as ORR methanol-tolerant in alkaline media. Bunazawa and Yamazaaki [62] tested Pd/C as cathode material in a single ADMFC. The performance of the single cell with Pd/C was comparable to that of the cell with Pt/C as cathode material. The ADMFC with Pd/C cathode did not only showed high performance, but also relatively high tolerance to methanol crossover. Kim et al. [163] investigated the ORR activity of Pt, Pd and Pd-Sn nanoparticles in CH_3OH-containing O_2-saturated KOH solution. The oxygen reduction current at Pt nanoparticles decreased and the onset potentials shifted in the negative direction in the presence of methanol. Pd nanoparticles showed a lower increase of the overpotential than Pt nanoparticles. This result indicates that Pd metal is more tolerant than Pt to the poisonous effect of methanol on the ORR activity. Conversely, both the magnitude of ORR current and the onset potential at Pd-Sn nanoparticles were unaffected by the addition of methanol. Pd-Sn nanoparticles exhibited a high methanol tolerance during the ORR in contrast to pure Pt and Pd catalysts. Surprisingly, notwithstanding Pd possess higher activity for ethanol oxidation in alkaline media than Pt [40], Jiang et al. [125] found that, when used as cathode catalyst, Pd has higher ethanol tolerance than Pt. The same researchers [164] investigated the simultaneous electro-oxidation of ethanol and electro-reduction of O_2 in O_2-saturated NaOH solutions on Pt-Ru/C and Pt/C catalysts. For the Pt/C, the ORR is suppressed by ethanol adsorbates at potentials lower than (0.05 V *vs.* $Hg/HgO/OH^-$ when both ethanol and oxygen are present in the solution. At potentials higher than (0.05 V, the EOR is suppressed by the ORR. The high EOR oxidation current on the Pt/C cathode would produce mixed potentials and degrade fuel cell performance. For the Pt-Ru/C, instead, the EOR has little influence on the ORR. Even in a 0.1 M ethanol solution, the EOR oxidation peak current of Pt-Ru/C is 6 times less than that of the Pt/C catalyst. At the typical cathode potential of 0.05 V, the ORR current in the presence of 0.1 M ethanol is almost similar to the ORR current in a pure O_2-saturated 0.1 M NaOH solution. According to the authors, these results indicate that Pt-Ru/C is an excellent ethanol-tolerant catalyst in an alkaline solution.

Demarconnay et al. [120] demonstrated the beneficial effect of bismuth towards ORR in alkaline medium when added to platinum. The $Pt_{0.8}Bi_{0.2}$/C appeared to be the best catalyst for oxygen reduction. This catalyst showed also a very good tolerance towards the presence of ethylene glycol.

The catalytic activity for oxygen reduction under the presence of ethylene glycol of carbon-supported $La_{1-x}Sr_xMnO_3$ (LSM/C) was investigated by Miyazaki et al. [165] by using a rotating disk electrode. The ORR activity on LSM/C was not influenced by the presence of EG in alkaline solution. This implies that LSM/C can be a promising candidate for cathode catalysts with high crossover tolerance. Tests in direct EG fuel cells supported this result.

Anode and alcohol-tolerant cathode catalysts for use in ADAFCs are reported in Table 1.

Table 1
Anode and cathode (alcohol-tolerant) catalysts for ADAFCs fuelled with different alcohols.

Fuel	Anode catalysts	Cathode catalysts (alcohol tolerant)
Methanol	Pt, Pt-M (M = Ru,Pd,Au), Pt-M_xO_y (M = Ce,Ni,V), Pt-$La_{1-x}Sr_xMO_3$ (M = Co,Mn), Ni, Ni-M (M = Ru,Cu), Ni-complex, Pd, PdNi, $AuLa_{1-x}Sr_xMO_3$ (M = Co,Cu), $La_{2-x}Sr_xNiO_4$, Ni-$La_{2-x}Sr_xNiO_4$	Fe-TMPP, Ag, Ag-W_2C, Pd, Pd-Sn
Ethanol	Pd, Pd-M (M = Ru, Au, Sn, Cu), Pd-M_xO_y (M = Ce, Zr, Mg, Co, Mn, Ni, In), Pd-(Ni-Zn), Pd-(Ni-Zn-P), Ru-Ni, Ru-Ni-Co.	Ag-W_2C, Pd, Pt-Ru
Ethylene glycol	Pt, Pt-M (M = Pb,Bi,Tl,Au), Au-M (M = Pb,Bi)	Pt-Pb, $La_{1-x}Sr_xMnO_3$

4. Alkaline anion exchange membranes (AAEMs)

4.1. A general overview

One of the main constraint of the alkaline fuel cells is the fact that the hydroxide ions of the electrolyte may react with the carbon dioxide, present in the oxidant gas stream, to form carbonate/bicarbonate according to the following reactions:

$$CO_2 + 2OH^- \rightarrow CO_3^{2-} + H_2O \quad (3)$$

$$CO_2 + OH^- \rightarrow HCO_3^- \quad (4)$$

The major cause of the degrading performance on CO_3^{2-}/HCO_3^- formation is the precipitation of large solid metal carbonate crystals in the electrolyte-filled pores of the electrode. Carbonates would block electrolyte pathways and electrode pores on platinum-based electrodes. These crystals not only block the pores, but also mechanically destroy the active layer [166]. Methanol produces CO_2 on electro-oxidation, and thus the problems related to CO_3^{2-}/HCO_3^- formation increase when methanol is used as the fuel in an alkaline fuel cell. Another disadvantage related to the use of a liquid electrolyte is the "electrode flooding" if the liquid is very abundant or, on the contrary, the "electrode drying" if the liquid leaks.

In order to overcome these difficulties and taking example on the electrolytes used in PEMFCs, solid polymer electrolyte (SPE) membranes were used in AFCs [167]. The use of alkaline anionic exchange membranes (AAEMs) may solve the problems due to the use of alkali, while allowing the electrokinetic vantages of alkaline fuel cells [166]. There are not mobile cations to precipitate solid crystals of metal carbonate, as with alkaline membranes the cations are immobilized on the polymer. Moreover, the ion transport within the membrane will be from the cathode to the anode. Unlikely to proton exchange membranes, water will be electro-osmotic transported from the cathode to the anode. As the water is now produced at the anode and consumed at the cathode, the water management regime is altered and potentially simplified [166]. Thus, the problem of the flooding at the cathode is avoided.

Many SPE membranes have been developed for both acid and alkaline fuel cell applications, and excellent reviews are present in literature [166,168]. For application in alkaline membrane fuel cells, values of the ionic conductivity >0.01 S cm^{-1} are mandatory. SPEs are typically divided into two classes, differentiated by the ionic mode of conduction within the polymer structure [167]: ion-solvating polymers (ISPs) and polyelectrolytes.

ISP membranes are ionically conductive solids based on the migration of cations or anions through the membranes. The polymer contains electronegative heteroatoms (such as oxygen, nitrogen, sulfur or phosphorus) which interact with the cations of the ionic salt by a donor-acceptor link. Polybenzimidazole (PBI) is the most commonly used ISP in PEMFCs. PBI has excellent thermochemical stability and mechanical properties. It is cheaper and has much lower permeability for hydrogen than Nafion®. Blank PBI is an electronic and ionic insulator, which becomes a very good ionic conductor when it is doped in proper conditions. However, compared with the acid-doped PBI, there is fewer reports about alkali-doped PBI for fuel cell applications. Xing and Savadogo [169] found that, when complexed with alkaline hydroxides PBI films show conductivities in the 5×10^{-5} to 10^{-1} S cm^{-1} range. The highest conductivity was obtained on 6 M KOH-doped PBI at 90 °C. In the presence of potassium carbonate, the conductivity of alkaline doped PBI decreases. This decrease in the conductivity may affect

the characteristics of fuel cells based on such membrane. The performance of the PEMFC with the KOH-doped PBI was similar to that of the PEMFC with Nafion®-117. Hou et al. [170,171] prepared and characterized alkali-doped PBI membrane for ADAFCs. PBI/KOH exhibited high thermal stability and acceptable mechanical properties. They found that free or combined KOH molecules may exist in the PBI matrix, which is helpful for the ionic conductivity of PBI/KOH.

Polyelectrolytes are polymers on which were grafted ionic functions (sulphonate, carboxylate or quaternary ammonium) on the skeleton of the polymer chain, ionic conductivity being ensured by the counter-ion. The most important example of polyelectrolyte is the Nafion® membrane which is extensively used in PEMFCs. A series of membrane materials have been tested for application in ADAFC, such as polysiloxane containing quaternary ammonium groups (PSQAS) [172], aminated poly(oxyethylene) methacrylates [173], quaternized cardo polyetherketone (QPEK-C) [174], quaternized cardo polyethersulfone (QPES-C) [175], radiation-grafted poly(vinylidene fluoride) (PVDF) and poly (tetrafluoroethene-co-hexafluoropropylene) (FEP) [176,177], and quaternized poly(phthalazinon ether sulfone ketone) (QAPPESK) [178].

4.2. AAEMs with high anion conductivity

Among AAEMs, fluorinated polymers seem the most promising materials for the use as AAEM in alkaline fuel cells. Varcoe et al. [176,179] developed thermally and chemically stable AAEMs by introduction of quaternary ammonium functionality via radiation-grafting onto FEP preformed membranes. These membranes exhibited conductivities between 0.010 and 0.035 S cm^{-1} in the temperature range 20–80 °C when fully hydrated. A significant problem with FEP-based AAEMs is the lack of physical strength; they tear easily and demonstrate critically poor durability when assembled in fuel cells. Thus, Varcoe and Slade [180] developed an AAEM where the FEP was replaced by a poly(ethylene-co-tetrafluoroethylene), ETFE, preformed film. This novel, physically strong, quaternary-ammonium-functionalised radiation-grafted (QAETFE) alkaline anion-exchange membrane showed promising H_2/O_2 and CH_3OH/O_2 fuel cell performances. The ETFE-based AAEM exhibited reduced physical swelling than both FEP-based AAEMs and Nafion®-115 membranes at 30 °C when fully hydrated. The normal OH^- conductivity of this AAEM was 0.030 ± 0.005 S cm^{-1} when fully hydrated (*i.e.* 32% of the H^+ conductivity of Nafion®); this represents an impressive level of conductivity for a solid alkaline ionomer with no additional incorporation of metal hydroxide species [181]. A full comparison between Nafion®-115 and the EFTE-based AAEM of the conductivities below 60 °C is displayed in Fig. 4 from ref. [182]. As expected, the AAEM showed lower conductivity than Nafion®-115. A problem with the application of AAEMs in direct methanol fuel cells is that the electro-oxidation of methanol, producing CO_2, would cause carbonation of the AAEM and this would lead to severely decreased conductivities. Therefore, the conductivities of the AAEM were investigated in the CO_3^{2-} anion form (ion exchanged with potassium carbonate rather than potassium hydroxide). As can be seen in Fig. 4, the conductivities are not significantly decreased in the CO_3^{2-} form compared to the OH^- form. Unfortunately, both FEP-based and ETFE-based AAEMs exhibited substantially lowered conductivities at lower relative humidities; this is undesirable for the anticipated application in alkaline membrane fuel cells, where operation with low humidity gases is considered necessary [181]. The case for development of AAEMs with conductivities that are less sensitive to humidity is therefore highlighted. Disadvantages of the fluorinated polymers are the complicated preparation procedures and the high material cost. Thus, many researchers attempted to develop cheaper non-fluorinated polymeric membranes.

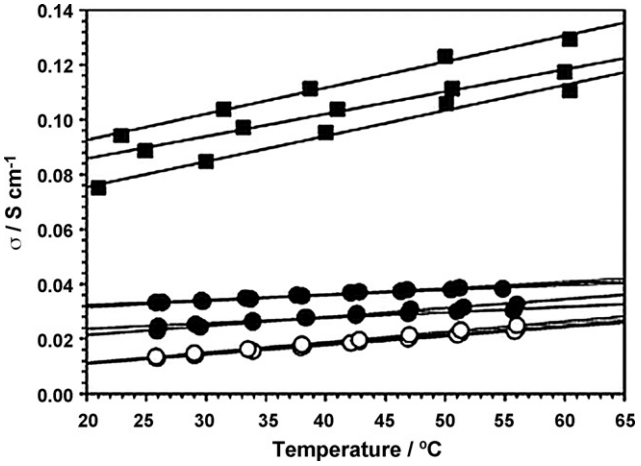

Fig. 4. Conductivities in water (fully hydrated), at increasing temperatures and determined using electrochemical impedance spectroscopy, of the ETFE-AAEM OH^- form (●, four replicate measurements), the ETFEAAEM in CO_3^{2-} form (○, three replicate measurements), and Nafion-115 in H^+ form (■, three replicate measurements). Reproduced from ref. [182], copyright 2007, with permission from the American Chemical Society.

Poly(vinyl alcohol) (PVA) is a low cost hydrophilic polymer. Yang et al. [183] prepared crosslinked PVA membranes using succinic acid (SSA) as the crosslinking agent. The crosslinked network of the PVA/SSA solid polymer membrane offers greater chemical and mechanical stability, reduces the degree of swelling and decreases the methanol crossover. A series of crosslinked quaternized polyvinyl alcohol (QAPVA) membranes were prepared by quaternizing PVA with (2,3-epoxypropyl) trimethylammonium chloride (EPTMAC), and then chemical crosslinking with glutaraldehyde (GA) [184]. Crosslinked QAPVA membranes have a weak mechanical strength. Their performance can be improved by several means, such as blending with inorganic materials or other polymers. Quaternized chitosan (HACC), the product of the reaction of chitosan and EPTMAC, has exchangeable OH^- anions arising from the quaternary ammonium groups in the matrix. HACC was chosen as the polymer material to blend with QAPVA to produce anion exchange membranes for application in alkaline fuel cells [185]. With the quaternary ammonium group grafted onto the matrix of QAPVA and HACC, the composite membranes have exchangeable anions. The composite membranes showed ionic conductivity in the range of 10^{-3} to 10^{-2} S cm^{-1}.

Poly(epichlorydrin-co-allyl glycidyl ether) copolymer is an aliphatic polyether, chemically stable in alkaline medium. It has an elastomer character with a low glass transition temperature ((25 °C) that permits stable mechanical properties up to 100 °C. The laboratory of Industrial Electrochemistry (CNAM) developed membranes based on this polyepichlorhydrin-based copolymer [167]. This copolymer was quaternized by 1,4-diazabicyclo[2.2.2]octane (Dabco) and both by Dabco and triethylamine (TEA). These membranes showed good electrochemical properties: ionic conductivity superior to 10^{-2} S cm^{-1} in KOH solutions, and anionic transport numbers between 0.95 and 0.99. Stoica et al. [186,187] prepared polymer electrolytes, using a poly(epichlorydrin-allyl glycidyl ether) copolymer as matrix. Anion conducting networks were obtained by the incorporation of two cyclic diamines, (DABCO) and 1-azabicyclo-[2.2.2]-octane (Quinuclidine). High conductivities were obtained, without any KOH addition, however ionic conductivity was particularly sensitive to relative humidity. The incorporation of a polyamide support considerably improved the mechanical properties without compromising ionic conductivity. These ionomers showed good thermal stability up to 220 °C. Some improvements might be considered such as the substitution of

the residual chloro function in the epichlorhydrin unit by some ether groups, which would improve the efficiency of the Cl^-/OH^- exchange performed directly on the membrane. Sollogoub et al. [188] consolidated these polyepichlorhydrin-based membranes by thermal or photochemical crosslinking. They found that the photochemical crosslinking is best adapted to the formation of the membranes, because of their greater thermal stability in the use temperature range. An alkaline fuel cell using this membrane was assembled, with performances reaching nearly 100 mW cm^{-2} at room temperature.

Among engineering plastics, poly(2,6-dimethyl-1,4-phenylene oxide) (PPO) is a unique material in view of its strong hydrophobicity, high glass transition temperature (T_g = 212 °C) and hydrolytic stability [189]. Despite the simplicity in structure when compared with other aromatic polymers, PPO can easily conduct many polymer-analogous reactions in both aryl- and benzyl-positions, such as electrophilic substitution on the benzene ring of PPO, radical substitution of the hydrogen from the methyl groups of PPO, and nucleophilic substitution of the bromomethylated PPO. It can be expected that these substituted materials have good miscibility since they all have PPO backbones. Therefore, to explore the miscible blend membranes for ADAFC, Wu et al. [190] prepared new composite anion-exchange membranes from the blends of chloroacetylated PPO (CPPO) and bromomethylated PPO (BPPO). The resulting membranes exhibited high hydroxyl conductivities (0.022–0.032 S cm^{-1} at 25 °C). The optimum composition of the blend membranes was 30–40 wt% CPPO. The properties of these CPPO/BPPO blend membranes can be remarkably improved by a simple heat treatment [191]. A partially inter-crosslinked structure can be formed therein via a Friedel-Crafts reaction without adding any crosslinking reagent or catalyst. Physical properties, such as toughness and thermal stability, are enhanced, owing to thermal treatment.

4.3. Highly stable organic–inorganic membranes

In addition to the low cost and high conductivity, the thermal, chemical and mechanical stability of the membrane is a key issue for its suitable use in a fuel cell. Organic–inorganic hybrid materials have been regarded as promising materials for many applications due to their unique performance to combine the remarkable functionality of organic materials with the stability of inorganic materials. Organic-inorganic hybrid membranes have been investigated for the use in low-temperature fuel cells. The introduction of an inorganic component into the polymer matrix enhances the mechanical strength and thermal stability of the membranes, and can influence their ionic conductivity and alcohol permeability. The addition of ceramic fillers, as hydrophilic nanocrystalline titanium oxide (TiO_2), hydroxyapatite ($Ca_{10}(PO_4)_6(OH)_2$, HAP) and montmorillonite ($(Na,Ca)_{0.33}(Al,Mg)_2(Si_4O_{10})(OH)_2 \cdot nH_2O$, MMT), into a polymer matrix serves to reduce the glass transition temperature (T_g) and the crystallinity, and to increase the amorphous phases of the polymer. When these fillers, used as stiffer materials, were added to the PVA matrix, the swelling ratio of the PVA/TiO_2, PVA/HAP and PVA/MMT composite polymer membranes was effectively reduced [192–194]. Further, the thermal property, dimensional stability and long-term cycle life was improved. The ionic conductivity of PVA/TiO_2, PVA/HAP and PVA/MMT composite hybrid membranes increased with the increase of the amount of ceramic fillers. Generally, when the fillers are added into the PVA polymer membrane, it shows more accessible free volumes (or more defect sites and voids) to retain the KOH electrolyte. Xiong et al. [195] prepared a series of organic-inorganic membranes, with SiO_2 contents of 5, 10 and 20 wt%, through sol–gel reaction of quaternized PVA with different contents of tetraethoxysilanes (TEOS). With the formation of networks by reaction of polymer matrix and silica, the thermal stability of the membrane was enhanced and the methanol permeability decreased. Holding water at high temperature, the conductivity of the hybrid membranes was improved. Among the hybrid membranes investigated, the hybrid membrane with a silica content of 5 wt% showed the lowest methanol permeability and the highest ion conductivity, 1.4×10^{-2} S cm^{-1} at 60 °C, higher than other QAPVA-based membranes at the same temperature. Wu et al. [196] prepared anion exchange hybrid membranes based on PPO through bromination, hydroxylation, quaternization, and sol–gel reaction with monophenyl triethoxysilane (EPh) or/and TEOS, followed by heat treatment at 120–140 °C for different times. Membranes treated at 130 °C for 2–10 h presented relatively high alkaline resistance and thermal stabilities: the thermal degradation temperature of membranes in the OH^- form was in the range of 156–170 °C, and the initial decomposition temperature reached up to 144 °C. These hybrid membranes showed conductivity values in the range of $1.0–8.5 \times 10^{-3}$ S cm^{-1}. Compared with the fluorinated-polymer-based AAEMs, the hybrid membranes have higher ion exchange capacities (IECs) and mechanical strength, comparable alkaline resistance and thermal stabilities, but lower swelling resistance and OH^- conductivity. In the next paragraph some AAEMs with low alcohol permeability are presented.

4.4. AAEMs with low alcohol permeability

Low alcohol permeabilities of AAEMs are mandatory because the use of thin membranes is necessary for minimised ionomer resistances and maximised water transport to the cathode catalyst sites. Therefore, it is crucial to evaluate the alcohol permeabilities of AAEMs, in order to assess their suitability for application in ADAFCs. Varcoe et al. [197] investigated the alcohol (methanol, ethanol and ethylene glycol) uptakes and permeability of two AAEMs, an ETFE-based radiation-grafted AAEM (AAEM-E) and a thicker commercial crosslinked quaternary ammonium-type AAEM (AAEM-C), and, for comparison, of a Nafion®-115 membrane. By the solvent uptake properties of the membranes, it was found that the AAEMs have a lower affinity towards methanol, ethanol and ethylene glycol than Nafion®-115; this was most evident for methanol. Nafion® showed a higher degree of swelling compared to the AAEMs for most solvents. The thickness increases with methanol were 47% for Nafion®, 20% for AAEM-C and 27% for AAEM-E; the corresponding values for ethanol were 49%, 22% and 30%, respectively. The situation with ethylene glycol is not so clear, particularly in view of the low swelling of Nafion® in this solvent (26%, 20% and 35% for Nafion®-115, AAEM-C and AAEM-E, respectively). Fig. 5 from ref. [197] presents the ex situ alcohol permeabilities for these polymer electrolyte membranes. The low alcohol contents for the AAEMs

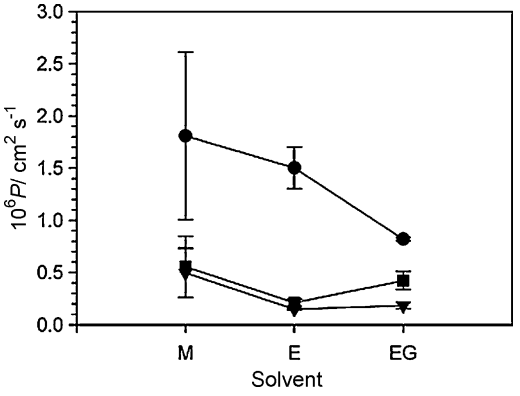

Fig. 5. Solvent permeabilities of AAEM-E (■), AAEM-C (▼) and Nafion®-115 (●) at room temperature. M = methanol, E = ethanol and EG = ethylene glycol. Reproduced from ref. [197], copyright 2007, with permission from Elsevier.

reported above have directly translated into desirably lower alcohol permeabilities compared to Nafion®. Ethanol permeabilities were lower than methanol permeabilities for all membranes, in agreement with previous studies, reporting lower ethanol permeabilities compared to methanol for Nafion® [198]. QPEK-C [174], QPES-C [175], QAPVA [184] and CPPO/BPPO [190,191] membranes showed lower methanol permeability than Nafion® membranes. In the case of crosslinked QAPVA the methanol permeability decreased with increasing the degree of crosslinking of the membranes. The crosslinking of QAPVA with GA forms compact structures, which resulted in an increase of the resistance to methanol crossover. In the same way, regarding the CPPO/BPPO membranes, their methanol permeability decreased following thermal treatment, owing to the formation of crosslinked structures [191]. Crosslinked QAPVA/HACC composite membranes showed smaller methanol permeability than crosslinked QAPVA membranes without chitosan [185]. The permeability of QAPVA/SiO_2 hybrid membranes [195] was lower than that of crosslinked QAPVA membranes [184], QAPVA-based composite membranes [185], and Nafion® membranes [198]. This indicates that silica is a good barrier to the methanol. The reaction of silica and polymer matrix forms a crosslinked network, reducing the channel allowing the passage of methanol molecules, so that the resistance to the diffusion of methanol is increased. However, the methanol permeability of the hybrid membranes increases with increasing silica content, since with the addition of silica, the self-polymerization of silica is dominant over the copolymerization of silica and QAPVA. The silica particles formed by the self-polymerization of silica destroy the continuous structure of the hybrid membranes and ease the passage of methanol through the membrane. Yang et al. [192] investigated the methanol, ethanol and 2-propanol permeability of PVA/TiO_2 hybrid membrane. The permeability of the PVA/TiO_2 composite membrane (in the order of 10^{-7} to 10^{-8} cm^2 s^{-1}) was much lower than that of the Nafion® membrane.

Hou et al. investigated the ethanol [170] and methanol [171] permeability of alkali-doped PBI membranes. Both methanol and ethanol permeabilities were much lower than that of Nafion®. The reason may be as follows: there are many hydrophilic groups of -SO_3H in H-Nafion® membrane, and Nafion® membrane is usually swollen more significantly than PBI and PBI/KOH in the presence of alcohol and water. The less expanded space among PBI backbones than that of Nafion® membrane probably resulted in lower alcohol permeability of PBI/KOH. Leykin et al. [199] observed that different doping levels of a PBI membrane correspond to different water content and thus can affect ethanol permeation. Ethanol crossover reached its maximum at approximately 3.5 M KOH. A further increase of alkali concentration led to a decrease of ethanol permeability.

The ionic conductivity and alcohol permeability of some AAEMs are reported in Table 2.

5. Tests in ADAFC

5.1. General overview

As previously reported, the reaction kinetics and catalytic activities of the anodic oxidation of alcohols and the cathodic reduction of O_2 in alkaline media are significantly higher than those in acidic media. With the recent development of polymeric membranes presenting a good anionic conductivity, the feasibility of using anion exchange membranes on fuel cells with alcohol as the fuel was investigated. Several tests on ADAFCs using an alkaline anion exchange membrane as the electrolyte have been reported [10,19,21,104,120,165,170,171,183,192,193,197,200–209]. The results suggest the potential application of anion exchange membranes in direct alcohol fuel cells. The first tests on ADAFCs with AAEM were carried out by Ogumi et al. [200] and Yu and Scott [19,201]. Ogumi et al. [200] investigated ADAFCs formed by Pt/C as anode and cathode catalysts, and a commercial ammonium-type anion exchange membrane (AHA) by Tokuyama Co. The fuel supplied was 1 M methanol or EG in 1 M KOH at 50 °C. Cell voltages were around 100 mV higher for EG compared to methanol. Yu and Scott [19] carried out fuel cell tests using the conventional hot-pressed MEAs with carbon supported Pt catalysts and a commercial quaternized crosslinked fluorinated polymer membrane (Morgane®-ADP, Solvay). Using 2 M methanol in 1 M NaOH as the fuel at 60 °C and a Pt loading of 2.1 mg cm^{-2} a maximum power density (MPD) of 11 mW cm^{-2} was attained. NaOH was added in the fuel stream because, as reported by Prabhuram and Manoharan [210], the MOR performance increases on going from a highly acidic range to a highly alkaline range. The same authors compared ADAFCs with platinised Ti mesh or Pt/C as the anode material, Pt/C as the cathode material and the Morgane®-ADP membrane at 60 °C in 2 M CH_3OH and 1 M NaOH and a similar Pt loading [201]. The cell with the platinised Ti mesh anode showed a higher MPD than that of the cell with Pt/C.

Matsuoka et al. [10] tested ADAFCs formed by Pt-Ru/C as anode catalyst, Pt/C or Ag/C as cathode catalyst, and the AHA membrane by Tokuyama Co. The cells operated at 50 °C, and were fuelled with four polyhydric alcohols and methanol for comparison. These alcohols (1 M) were dissolved in 1 M KOH aqueous solution. The maximum power densities were in the order of ethylene glycol > glycerol > methanol > erythritol > xylitol. The direct ethylene glycol fuel cell showed the highest power density. Alkaline direct alcohol fuel cells using silver as a cathode catalyst showed good performance, however the open circuit voltage of a cell with a silver catalyst was ca. 150 mV lower than that of a cell with a platinum catalyst under the same conditions. The performance of alkaline direct ethylene glycol fuel cells using Ag/C was improved by increasing the concentration of ethylene glycol. The performance of a cell with 3 or 5 M ethylene glycol solution was comparable to that of a cell using Pt/C catalyst in the large current density region (>40 mA cm^{-2}). Couteanceau et al. [21] tested alkaline direct alcohol fuel cells, fuelled with methanol (ADMFC) and ethylene glycol (ADEGFC), using Pt/C 40% as anode and cathode catalyst and the Morgane®-ADP membrane. They demonstrated the necessity to add sodium hydroxide to methanol and EG aqueous solutions in order to obtain significant performance. 4 M of NaOH added seems to be an optimum value, and a maximum of 18 mW cm^{-2} was observed at room temperature. In the case of the ADEGFC, with a concentration of 2 M ethylene-glycol and 4 M sodium hydroxide, a maximum of 19 mW cm^{-2} of power density was obtained at 20 °C, a value very closed to that observed for methanol. In addition to the previous works, further papers addressed to the use of ethylene glycol as the fuel in ADAFCs [104,120,165]. Different anode and cathode catalysts were tested. The best results were obtained using a ternary Pt-Pb-Pd/C catalyst as anode material [104], and a binary Pt-Pb/C catalyst as cathode material [120].

In all the previous works, commercial quaternized membranes were used as solid electrolyte in ADAFCs. In the following part of this paragraph tests on ADAFCs prepared using homemade AAEMs are reported. Varcoe and Slade [180] prepared ADMFCs using a homemade quaternized ETFE-based membrane and PtRu and Pt black as anode and cathode materials, respectively. Moreover, unlike from the previous ADAFC tests, aqueous methanol without MOH added was used as the fuel. Peak power densities of 1.5 mW cm^{-2} at 50 °C increasing to 8.5 mW cm^{-2} at 80 °C (with additional reactant pressurisation) were obtained. According to the authors, these results represent the highest peak power performances obtained with metal cation-free quaternary-ammonium-functionalised alkaline-membrane-MEAs and demonstrate that the presence of M^+OH^- in an aqueous

Table 2
Ionic conductivity and alcohol permeation of some AAEM and Nafion 115.

Fuel	Membrane	Ionic conductivity/S cm^{-2}	Alcohol permeability/P cm^2 s^{-1}	Ref.
Methanol	radiation-grafted ETFE-AAEM	3.0×10^{-2} (30 °C)	0.6×10^{-6} (20 °C)	[197]
Ethanol			0.3×10^{-6} (20 °C)	
EG			0.5×10^{-6} (20 °C)	
Methanol	QPEK-C	1.6×10^{-3} (20 °C) 5.1×10^{-3} (60 °C)	$P < 10^{-9}$ (30 °C)	[174]
Methanol	QPES-C	4.1×10^{-2} (25 °C) 9.2×10^{-2} (70 °C)	5.72×10^{-8} (25 °C) 1.23×10^{-7} (70 °C)	[175]
Methanol	Crosslinked QAPVA	$2.7–7.3 \times 10^{-3}$ (30 °C)	$(1.0\text{-}4.1) \times 10^{-6}$ (30 °C)	[184]
Methanol	Crosslinked QAPVA/HACC	$0.3–1.3 \times 10^{-2}$ (60 °C)	$0.6–4.4 \times 10^{-6}$ (30 °C)	[185]
Methanol	QAPVA/SiO_2	$3.5–6.8 \times 10^{-3}$ (30 °C)	$0.9–1.2 \times 10^{-6}$ (30 °C)	[195]
Methanol	PVA/TiO_2	$0.3–4.8 \times 10^{-2}$ (30 °C)	3.7×10^{-7} (25 °C)	[192]
Ethanol			2.8×10^{-7} (25 °C)	
Methanol	CPPO/BPPO	$2.2–3.2 \times 10^{-2}$ (25 °C)	$1.4\text{-}1.5 \times 10^{-7}$ (25 °C)	[190]
Methanol	Crosslinked CPPO/BPPO	$2.2–3.2 \times 10^{-2}$ (25 °C)	$1.0–1.3 \times 10^{-7}$ (25 °C)	[191]
Methanol	PBI	1.8×10^{-2} (25 °C)	2.6×10^{-7} (25 °C)	[171]
Ethanol	PBI	1.8×10^{-2} (25 °C)	6.5×10^{-7} (25 °C)	[170]
Ethanol	PBI	–	$2.5–8.6 \times 10^{-8}$ (25 °C)	[199]
Methanol	Nafion 115	9.3×10^{-2} (30 °C)	1.9×10^{-6} (20 °C)	[197]
Ethanol			1.6×10^{-6} (20 °C)	
EG			0.9×10^{-6} (20 °C)	

methanol fuel is not needed to obtain a functioning ADMFC. Yang et al. [183] tested an ADMFC composed of MnO_2/BP2000 as the cathode catalyst, PtRu black as the anode catalyst and an alkaline crosslinked non-quaternized PVA/SSA membrane. The MPD of the ADMFC goes from 2.38 mW cm^{-2} at 30 °C to 4.13 mW cm^{-2} at 60 °C and 1 atm in 2 M KOH + 2 M CH_3OH solution. The ADMFC with the same catalysts but a hybrid membrane, obtained by adding ceramic fillers such as TiO_2 and HAP to PVA, better performed than the cell with PVA only. The MPD of the ADMFC increased from 2.38 to 9.25 mW cm^{-2} using PVA/TiO_2 [192], to 11.48 mW cm^{-2} using PVA/HAP [193]. Regarding the ADAFC with the PVA/TiO_2 hybrid membrane fuelled with different alcohols, the MPDs were also in the order of methanol > ethanol > 2-propanol. It has to be remarked, however, that Pt-Ru is the best catalyst for the MOR in alkaline media, while the best catalyst for the EOR is Pd. This should explain the better performance of ADMFC than that of ADEFC. Summarizing, these ADAFCs consisting of a low cost air cathode electrode (MnO_2 is a non-precious metal catalyst), a Ti-based Pt-Ru anode electrode and a PVA-based solid polymer membrane (PVA is a cheap non-perfluorosulfonated polymer membrane, as compared to the expensive Nafion® membrane) can be considered a low cost system, with respect to the acidic DAFC.

Table 3
Performance, as maximum power density (MPD), of some Pt-containing ADAFCs with different catalysts and AAEMs. Only temperature is reported in operating conditions, but it has to be remarked that MPD depends also on other parameters such as catalyst loading, gas flow, pressure.

Fuel	Anode	Cathode	Electrolyte	Temperature (°C)	MPD (mW cm^{-2})	Ref.
Methanol + KOH	Pt/C	Pt/C	AHA Tokuyama	50	5.5	[200]
EG + KOH					9.2	
Methanol + NaOH	Pt/C	Pt/C	Morgane®-ADP, Solvay	60	6.8	[19]
Methanol + NaOH	Pt/Ti	Pt/C	Morgane®-ADP, Solvay	60	7.8	[201]
Methanol + KOH	Pt-Ru/C	Pt/C	AHA Tokuyama	50	6.2	[10]
EG + KOH (1 M)		Pt/C			9.5	
EG + KOH (3 M)		Ag/C			8.1	
Methanol + NaOH	Pt/C	Pt/C	Morgane®-ADP, Solvay	20	18	[21]
EG + NaOH					19	
EG + NaOH	Pt/C	Pt/C	Morgane®-ADP, Solvay	20	19	[104]
	PtPb/C				22	
	PtPbPd/C				28	
EG + NaOH	Pt/C	Pt/C	Morgane®-ADP, Solvay	20	19	[120]
		PtPb/C			23.5	
EG + KOH	PtRu/C	Pt/C	A-006, Tokuyama	80	25	[165]
		Ag/C			20	
		LaSrMnO/C			18	
Methanol	PtRu	Pt black	QAETFE	50	1.5	[180]
				80	8.5	
Methanol + KOH	PtRu black	MnO_2/C	PVA/SSA	30	2.38	[183]
				60	4.13	
Methanol + KOH	PtRu black	MnO_2/C	PVA/TiO_2	25	9.25	[192]
Ethanol + KOH					8.0	
Methanol + KOH	PtRu black	MnO_2/C	PVA/HAP	25	11.48	[193]
Ethanol + KOH	PtRu/C	Pt/C	PBI/KOH	75	49.20	[170]
				90	60.95	
Methanol + KOH	PtRu/C	Pt/C	PBI/KOH	90	31	[171]
Methanol	PtRu	Pt black	AAEM-C	50	1.17	[197]
Ethanol					1.71	
EG					1.57	
Ethanol + KOH	PtRu	Pt black	AAEM, Tokuyama	20	58	[202]
Methanol + KOH	PtRu/C	Pt/C	AAEM, Tokuyama	20	6.8	[203]

Hou et al. prepared ADAFCs with Pt-Ru/C as the anode catalyst, Pt/C as the cathode catalyst, and KOH-doped PBI as the anionic exchange membrane, then these cells were tested at 90 °C using a KOH + ethanol [170] or methanol [171] solution. The PBI/KOH membrane exhibited excellent endurance both in basic solution and at higher temperature. The maximum power densities of ADEFC and ADMFC were about 61 and 31 mW cm^{-2}, respectively. The much lower performance of ADMFC than that of ADEFC under the same conditions should be attributed to the presence of CO_2, formed by complete methanol oxidation in the ADMFC, which reacts with KOH, causing carbonation of the membrane and collapsing electrode pores. Conversely, ethanol tends to be oxidized incompletely, because most of the C–C bonds cleavage in ethanol molecule cannot take place, minimizing the negative effect of carbonation.

The performances of ADAFCs with different catalysts and membranes are reported in Table 3.

5.2. Comparison between alkaline and acid direct alcohol fuel cells

In some papers the performance of alkaline fuel cells with anion exchange membranes has been compared with that of acid fuel cells with proton exchange membranes. Varcoe et al. [197] tested three ADAFCs formed by Pt-Ru as anode catalyst, Pt black as cathode catalyst, by two AAEM, an ETFE-based radiation-grafted AAEM (AAEM-E) and a thicker commercial crosslinked quaternary ammonium-type AAEM (AAEM-C), and, for comparison, by a Nafion®-115 membrane. All the types of cells were fuelled with aqueous solutions of methanol, ethanol and ethylene glycol. Poorer power densities of alkaline DAFCs were observed with respect to the performances of the acid DAFCs, and were due overall to the absence in OH^- in the fuel stream. The power performance substantially decreased with the Nafion®-containing cells when replacing methanol with ethanol and ethylene glycol. Conversely, the AAEM-based cells exhibited no such decrease in peak power densities: higher MPDs were observed with the C_2 alcohols on testing of the thicker AAEM. Fujwara et al. [202] compared the performance of a direct ethanol fuel cell with a Pt-Ru anode and a Pt cathode using an anion exchange membrane (AAEM, Tokuyama Co.) with a direct ethanol fuel cell with the same catalysts and a cation exchange membrane (CEM, Nafion®-117). The cell voltage and power density versus current density of AEM- and CEM-type DEFCs are shown in Fig. 6. The maximum power density of the cell significantly increased from 6 to 58 mW cm^{-2} at room temperature and atmospheric pressure when the electrolyte membrane was changed from CEM to AAEM. The anode and cathode polarization curves showed a decrease in the anode potential and an increase in the cathode potential for the cell with AAEM compared to the cell with CEM. Kim et al. [203] compared the performance of direct methanol fuel cells using alkaline and acid exchange membranes. In both the cells the anode was Pt-Ru/C and the cathode Pt/C. The cell with AAEM exhibited a higher open circuit voltage and superior cell performance than those in cell using Nafion® 117. In 1 M methanol solution, the MPD of the cell with AAEM was 6.8 mW cm^{-2} while that of the cell with Nafion®-117 was 5.2 mW cm^{-2}. In addition, by using home-made Pd-Sn/C catalyst as a cathode catalyst on ADMFC, the membrane electrode assembly (MEA) using Pd-Sn/C catalyst as cathode showed a higher performance than the usual commercially available Pt/C catalyst in high methanol concentration.

5.3. Pt-free ADAFCs

Considering the high cost and the limited availability of platinum, the development of Pt-free fuel cells is necessary. Very recently, tests were carried out on Pt-free ADAFCs [204–209], in particular on cells with Pd-based catalysts as anode materials and ethanol as the fuel, being Pd the best catalyst for ethanol oxidation. These ADAFCs presented high performance, and, particularly, Bianchini et al. [204] reported exceptionally high values of power density (55 mW cm^{-2} at 20 °C and 170 mW cm^{-2} at 80 °C) for the ADEFC formed by a Tokuyama A-006 anion-exchange membrane, Pd-(Ni-Zn)/C as anode catalyst and Fe-Co as cathode catalyst. Ethanol oxidation occurs by the selective conversion of ethanol into potassium acetate with negligible formation of CO_3^{2-}, avoiding in this way catalyst poisoning or membrane carbonation. For comparative purposes, electrodes coated with Pd/C were successfully used to selectively oxidize ethanol to acetic acid in alkaline media in both half cells and ADEFC, yet neither the power output (28 mW cm^{-2} at 20 °C and 120 mW cm^{-2} at 80 °C) nor the electrochemical stability were comparable to those exhibited by the Pd-(Ni-Zn)/C electrode. This finding suggests that the Ni–Zn alloy exerts a beneficial action on the activity of the Pd sites. Also, Modestov et al. [205] attained a power density of about 100 mW cm^{-2} at 80 °C with an ADEFC formed by Ru-V/C as anode catalyst, Co-TMPP as cathode catalyst and a KOH/PBI membrane. The performance of this ADEFC single cell was remarkably higher than that of the ADEFC, employing the same KOH/PBI membrane and Pt-based electrodes (61 mW cm^{-2} at 90 °C) [170]. Finally, it has to be promptly pointed out that the corresponding acid DEFCs, with more expensive Pt-based catalysts, exhibit MPD values lower than 100 mW cm^{-2}. Very recently, Shen et al. [206] tested an ADEFC formed by a Tokuyama A-201 anion-exchange membrane, Pd/C or Pd_2Ni_3/C, synthesized by simultaneous Pd and Ni reduction using $NaBH_4$, as anode catalyst and non-platinum HYPERMEC™ catalyst by Acta as cathode catalyst. The measurements were made by feeding 1.0 M ethanol/1.0 M KOH and 3.0 M ethanol/5.0 M KOH to the fuel cell at 60 °C. In both conditions, the ADEFC with a Pd_2Ni_3/C anode better performed than that with Pd/C in terms of both open-circuit voltage (OCV) and power density. By feeding 3.0 M ethanol mixed with 5.0 M KOH, the cell with the Pd_2Ni_3/C catalyst as an anode, the OCV was 0.89 V and the peak power density was 90 mW cm^{-2}, while in the case of Pd/C, the OCV was 0.79 V and the peak power density was 67 mW cm^{-2}.

The performances of some platinum-free ADAFCs are reported in Table 4.

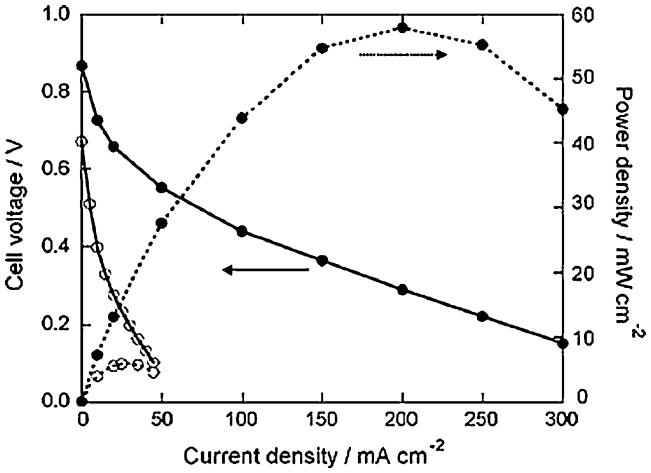

Fig. 6. Cell voltage and power density versus current density plots of DEFCs using an AEM and 1 M ethanol + 0.5 M KOH solution (●) or a CEM and 1 M ethanol aqueous solution (○), as an electrolyte membrane and a fuel, respectively, at room temperature and atmospheric pressure. Anode: 3 mg cm^{-2} PtRu black, cathode: 3 mg cm^{-2} Pt black, and cathode gas: humidified O_2.
Reproduced from ref. [202], copyright 2008, with permission from Elsevier.

Table 4
Performance, as maximum power density (MPD), of some Pt-free ADAFCs with different catalysts and AAEMs.

Fuel	Anode	Cathode	Electrolyte	Temperature (°C)	MPD mW cm^{-2}	Ref.
Ethanol + KOH	Pd–(Ni–Zn)/C	Fe-Co HYPERMEC™	A-006, Tokuyama	20 80	58 170	[204]
Ethanol + KOH	RuV/C	Co-TMPP/C	PBI	80	90 air 110 O_2	[205]
Ethanol (1 M) + KOH (1 M) Ethanol (3 M) + KOH (5 M)	Pd_2Ni_3/C	Fe-Co HYPERMEC™	A201, Tokuyama	60 60	44 90	[206]
Ethanol + KOH	Ni–Fe–Co HYPERMEC™	Fe-Co HYPERMEC™	A201, Tokuyama	40	60	[207]
Methanol + KOH Ethanol + KOH EG + KOH	Pd/MWCNT	Fe-Co HYPERMEC™	A-006, Tokuyama	20–22	7 18 5	[208]

5.4. Presence of OH^- in the fuel stream

As previously reported, generally MOH (M = K, Na) was added in the fuel stream because the activity for alcohol oxidation on different catalysts increases on going from an acidic range to an alkaline range. Beden et al. [23] studied the MOR on a platinum electrode in 10^{-3}, 10^{-2}, 10^{-1}, 0.5 and 1 M NaOH solutions with different concentrations of methanol (10^{-3}, 10^{-2}, 10^{-1} and 1 M CH_3OH). They observed an increase in the MOR activity as the hydroxyl ion concentration in solution is increased for a given methanol concentration, and a decrease in the MOR activity once the hydroxyl/methanol concentration ratio is greater than unity. Analogously, Prabhuram and Manoharan [210] investigated the MOR activity on platinum electrodes in electrolytes containing different concentrations of alkali (1, 6 and 11 M KOH) and methanol (1, 6 and 11 M CH_3OH). They reported that methanol oxidation on Pt electrodes increases only up to 6 M KOH solution. At higher concentrations, the activity declines. Also, they observed that the MOR performance depends on the methanol concentration of a given pH solution. The 6 M KOH/6 M CH_3OH mixture yields the highest MOR performance. It appears that CHO species do not become bonded on the platinum electrodes in the equimolar mixture 6 M KOH/6 M CH_3OH. They concluded that by choosing the proper ratio of OH^- ions and CH_3OH, it is possible to remove completely the intermediate organic species and/or poisonous species that retard the MOR rate on the electrode surface. Yu et al. [211] found that the activity of methanol oxidation on Pt/Ti in aqueous alkaline systems increased with pH or OH species coverage on the electrode surface. A reaction order of close to 0.5 was obtained for both NaOH and CH_3OH/NaOH solutions indicating that adsorption of methanol and OH^- on the platinised electrode follows Termkin isotherm. In the high potential region, a poisoning effect was observed at CH_3OH/OH^- concentration ratio greater than 1, which could have arisen from an excess of methanol at the electrode surface and/or depletion of OH^- at the electrode surface. The onset potential for methanol oxidation varied with the concentration of NaOH, shifting cathodic with increasing NaOH concentration from 0.1 to 2 M, at a fixed 2 M CH_3OH solution. All the mentioned studies were performed in a half-cell. However, in an ADMFC, i.e. in the presence of an anionic exchange membrane, the effect of OH^- and hydroxyl/methanol concentrations can be different. According to Coutanceau et al. [21], taking into account that the anionic membrane used in ADMFC is an ionic conductor needing a constant concentration of OH^- to maintain its conductivity, the amount of added sodium hydroxide is a critical point. If it is not sufficient, some hydroxyl species would be taken from the membrane to form carbonate and the conductivity of the membrane will drop rapidly. However, if the concentration of OH^- is too high, it becomes difficult to stabilize working conditions of the ADMFC and the observed performances decrease rapidly with time. To investigate an effect of ion conductivity on cell performance, Kim et al. [203] investigated the behavior of an ADMFC operating with various KOH concentrations in anode fuel. Fig. 7 from ref. [203] shows the polarization curves of an ADMFC operating with 2 M CH_3OH and various KOH concentrations. The current density at a cell voltage of 0.1 V increased from 39 to 65 mA cm^{-2} as KOH concentration solution increases from 1 to 3 M. Moreover, the MPD in 3 M KOH was about two times larger than that in 1 M KOH, from 5.9 to 11.5 mW cm^{-2}. In the same way, Li et al. [209], to study the influence of the electrolyte on ADEFC performance, tested 1.0 and 5.0 M ethanol aqueous solutions with various KOH concentrations. From polarization curves for different KOH concentrations ranging from 1.0 to 11.0 M at a fixed ethanol concentration of 1.0 M, they observed that the voltage increases with increasing KOH concentration in the low current density region (lower than 150 mA cm^{-2}). This suggests that in the low current density region, the concentration of OH^- ion is the predominant factor that determines the anode potential. This result was further confirmed by the increase of the OCV with increasing KOH concentration. It has to be pointed out that the increase in KOH concentration is limited by its solubility in ethanol solutions. With an ethanol concentration of 1.0 M, the KOH concentration cannot be higher than 13.0 M. Unlike the results obtained in the low current density region, in the high current density region, when the KOH concentration is increased above 5.0 M, the voltage falls. Similar results were obtained by increasing the ethanol concentration to 5.0 M. Regarding the ADEGFCs, also if MOH is commonly added in the fuel stream, analogous detailed investigations are not present in literature.

On the other hand, Varcoe et al. [166] asserted that the addition of MOH into the fuel stream is not desirable for two principal reasons: (1) The MOH constitutes a further chemical component reducing the energy density of the fuel and making this fuel supply highly caustic. (2) The presence of M^+ in the system will lead to the formation of precipitates of carbonate/bicarbonate on reaction of the OH^- with CO_2.

5.5. Effect of the polymer binder in the catalyst layer

In preparing the electrodes for low-temperature fuel cells that use membrane electrolytes, a polymer binder is essential to bind discrete catalyst particles to form a porous catalyst layer that simultaneously facilitates the transfer of ions, electrons and reactants/products. Firstly, polytetrafluoroethylene (PTFE) was used as the binder in the catalyst layer of PEMFCs, but PTFE does not conduct protons. The substitution of PTFE with Nafion®, which is a perfluorosulfonic acid polymer with high proton conductivity, was a decisive pathway in the development of the low-temperature fuel cell technology [212]. In acidic fuel cells, Nafion® has proved to be the best binder for both the anode and cathode catalyst layers. Regarding the ADAFCs, PTFE or Nafion® was added to the cata-

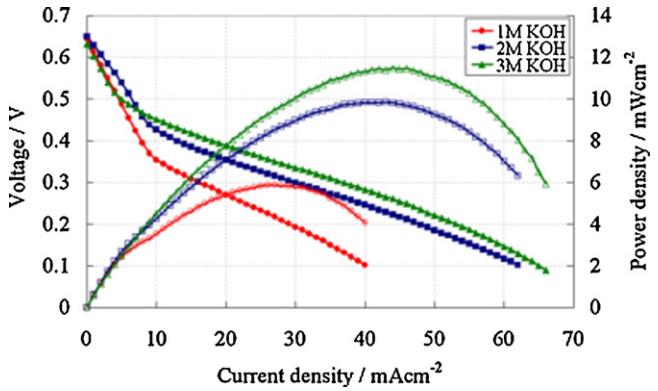

Fig. 7. Polarization curves of MEA with anion exchange membrane (Tokuyama Co.) (anode: PtRu/C, 1.8 mg cm^{-2}, anionic ionomer: 28%; cathode: Pt/C, 2.0 mg cm^{-2}, anionic ionomer: 27%), in 2 M CH3OH containing various concentration of KOH (1 M (● and ○), 2 M (■ and □), and 3 M (▲ and △)).
Reproduced from ref. [203], copyright 2009, with permission from Elsevier.

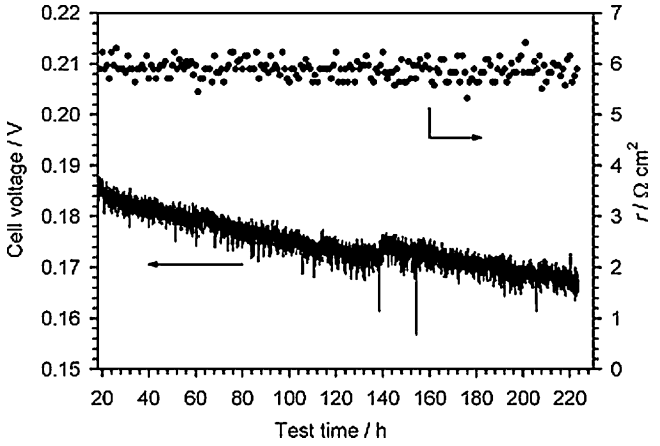

Fig. 8. Medium-term test with an AAEM-MEA (4 mg cm^{-2} Pt-Ru anode and 4 mg cm^{-2} Pt black cathode both with the alkaline interface). Test conditions: 50 °C, 0.1 A discharge, cathode: 2 dm^3 min^{-1} air (RH = 100%), anode: methanol (2 M, 2 cm^3 min^{-1}), no back pressures.
Reprinted from ref. [11], copyright 2006, by permission of The Royal Society of Chemistry.

lyst layer to serve as a binder [19–21]. Although both PTFE and Nafion® can bind catalyst particles so as to form a catalyst layer, they cannot conduct hydroxide ions. Hence, these two polymer materials are not a good choice as the binder for preparing MEAs for ADAFCs. Recently, an anion-conducting ionomer, named A3, has been developed by Tokuyama as a binder for ADAFCs, and the effect of the presence of A3 in the catalyst layer on cell performance has been investigated [203,206,213]. Kim et al. [203] prepared MEAs with various contents of A3 in the anode catalyst layer to evaluate the effect of the ion conductivity of the catalyst layer. The MPD of ADMFCs fuelled with 1 M CH_3OH containing 1 M KOH increased with increasing ionomer content in the anode catalyst layer (in the range 10–35 wt%). In the same way, Bunazawa and Yamazaki [213] investigated the influence of A3 content in the anode and cathode catalyst layers of ADMFCs. The ionomer contents of MEAs were 30, 39.2, 45.4 and 51.7 wt% both for the anode and the cathode. The MEA with 45.4 wt% of ionomer content showed the highest performance when both non-alkaline (CH_3OH (1 M)) and alkaline (CH_3OH (1 M) + NaOH (0.5 M)) fuels were used. Comparing to the MEA with 45.4 wt% of ionomer, the MEA with 39.2 wt% of ionomer showed higher OCV, but the *I–V* curve was sharp. This indicates that the OH^- transfer of this MEA was low because of the low ionomer content. On the other hand, MEAs with 51.7 and 56.3 wt% of ionomer showed higher activation polarization because the ionomer content was at a surplus, and the reactant supply was impeded. Unlikely the results previously reported [203,213], Li et al. [206] observed that in the presence of KOH in the fuel, the ADEFC performance decreased with increasing A3 content in the catalyst layer from 0 to 30 wt% over the whole current density region, including the activation, ohmic and concentration-controlled regions. The maximum current density was 65 mA cm^{-2} with 30 wt% A3, whereas it was 138 mA cm^{-2} without ionomer in the anode catalyst layer. According to the authors, as film-like structures are likely formed when A3 is incorporated into the catalyst layer, the active sites may be covered by A3 films, leading to a decrease in the active surface area. The A3 films also increase the transport resistance of hydroxide ions, electrons and fuel in the catalyst layer. When the anode was fed with 3 M ethanol solution without added KOH, the cell performance varied with ionomer content, and the best performance was achieved with 10 wt% of ionomer. The use of the A3 ionomer could extend the active surface area of the anode catalyst layer as it can conduct hydroxide ions, which is beneficial to anode performance. On the other hand, excessive A3 ionomer in the anode catalyst layer hinders the transfer of ethanol and electrons to catalytic sites and thus lowers the anode performance.

5.6. Duration tests.

Long-term durability of MEAs is always a question for any fuel cell and in particular in the case of the ADAFCs, where one of the major causes of the degrading performance is the precipitation of large solid metal carbonate crystals, formed by the interaction of hydroxide ions with carbon dioxide; either in the air stream or formed as part of fuel oxidation, in the electrolyte-filled pores of the electrode. However, few tests on durability have been carried out on ADAFCs. Moreover, it is important to remark, these studies were performed without MOH presence in the system [11,21] or without CO_2 formation by alcohol oxidation [204], i.e. in the absence of carbonation. Varcoe et al. [11] carried out a 233 h durability test on a ADMFC, formed by an alkaline crosslinked quaternized poly(vinylbenzyl)-based membrane, and by Pt-Ru and Pt blacks as anode and cathode catalysts, respectively, and fuelled with a 2 M CH_3OH aqueous solution. As can be seen in Fig. 8, the cell voltage stabilized to a very low degradation rate of 95 ± 10 μV h^{-1} (with no associated increase in cell area resistance). After this 233 h test, the methanol/O_2 performance was re-evaluated, and the MPD increased from 0.9 to 1.1 mW cm^{-2}, indicating that performance was recoverable. The ion-exchange capacity of the membrane after the 233 h test had reduced by less than 5%. In contrast, the performance of a KOH electrolyte AFC (6 mol dm^{-3}) degraded rapidly over the course of 70 h at 60 °C and 94 h at 30 °C, due to carbonate precipitation at the anode, when fuelled with methanol. According to the authors, the above observations demonstrate that elimination of M^{n+} cations in such systems minimizes performance losses due to carbonation, thereby allowing alcohols to be used in AFCs. In the same way, Scott et al. [21] tested the stability of an ADMFC, formed by a Morgane®-ADP hydroxide ion conducting membrane, and Pt-Ru/C and Pt/C as catalysts, and fuelled with an aqueous solution of CH_3OH. The cell was tested for 12 days at a fixed current density (20 mA cm^{-2}) at 60 °C without any significant loss in performance. Bianchini et al. [204] performed a galvanostatic experiment at 60 °C on an ADEFC formed by a Tokuyama A-006 anion-exchange membrane, Pd-(Ni-Zn)/C and Fe-Co as anode and cathode catalysts, respectively, and fuelled with a 2 M KOH solution of ethanol. After a conditioning time of 1 h at the OCV of 0.75 V, the cell was held to a constant current density of 20 mA cm^{-2} for 217 h showing a modest 15% decay of the cell voltage. The high stability of this ADEFC has to be ascribed to negligible formation of carbonate, as detected by NMR, which is consistent with the selective acetate formation (no

C–C bond cleavage) on the anode side and negligible atmospheric CO_2 uptake on the cathode side.

6. Conclusions

Alkaline direct alcohol fuel cells have potential advantages, compared to acidic alcohol fuel cells. First, electrocatalytic reaction of alcohol oxidation and oxygen reduction reaction in alkaline media are more facile than in acidic media, allowing to use low catalysts loadings and to select a wide range of catalysts, e.g. non-precious metals. Second, it is possible to reduce the alcohol crossover, because the conducting pathway of OH ions from the cathode to the anode through the membrane is opposite to the direction of the electro-osmotic drag. Reduced alcohol crossover will allow the use of thinner membranes, improving fuel cell performances. In addition, water management can be easily performed in accordance with reduction of flooding at the cathode. When OH ions are present in the fuel stream, comparison between an alkaline and an acidic direct alcohol fuel cell, both using the same catalysts, indicates a better performance of the former, independently of the type of fuel [202,203].

On the basis of the performances of various types of ADAFCs, the most relevant observation is the mandatory presence of OH ions in the fuel stream. Up to date, in the absence of OH^- in the alcohol solution the cell performance is very poor and far from a possible industrial application. The addition of MOH into alcohol supply, however, is not desirable for different reasons, such as corrosion, electrode weeping, mechanic electrode destruction by carbonate crystals and catalyst decomposition [214]. Therefore, in addition to short-time tests, durability tests on ADAFCs fuelled with alcohol + MOH in the presence of CO_2 have to be carried out, to find a MOH content, resulting in a good compromise between the positive effect on cell performance and the negative effect on the durability.

Generally, the presence of an anionic binder in the catalyst layer improves the cell performance, and the optimum ionomer content goes through a maximum. However, as film-like structures are likely to form when the ionomer is incorporated into the catalyst layer, the active sites may be covered by ionomer films, leading to a decrease in the active surface area, and, as a consequence, in the cell performance.

The comparison of the performance of ADAFCs, formed by the same catalysts and membrane but fuelled with different fuels, to establish a ranking of fuels is hazardous, considering that the activity for alcohol oxidation depends on the anode catalyst. The correct comparison should be carried out using the best catalyst for each fuel, and not the same catalyst for all the fuels compared! Regarding the comparison of methanol with ethanol, unlike acidic direct alcohol fuel cells, where DMFC performance » DEFC performance, in alkaline media ADEFC performance ≥ ADMFC performance (notwithstanding the use of Pt-based anode catalysts, being Pd the best catalyst for the EOR in alkaline media) [170,171,192,197]. Indeed, using Pd as anode catalyst ADEFC performance » ADMFC performance [207]. Regarding ADAFCs with Pt-based anode catalysts, fuelled with methanol and ethylene glycol, the performance of ADEGFCs was higher than that of ADMFCs [10,21,197,200]. Summarizing, in direct alcohol fuel cells the choice of the liquid fuels at the anode can be expanded to include alcohols other than methanol.

The increasing interest on ADAFCs is strictly related to the development of AAEMs. In recent years many researchers focused on preparation of anion exchange membranes with both lower methanol permeability and manufacturing cost than those of Nafion®. A series of membranes have been thus reported for application in DMAFC, and almost all showed lower alcohol permeation than Nafion®! However, AAEMs have two intrisic defects, 1) low ionic conductivity because the mobility of OH^- is only 1/3–1/2 of that of H^+. For example the conductivity of commercial anion-exchange membrane Morgane®-ADP was reported to be 1/3 that of Nafion® membranes (Nafion: proton conductivity ~0.08 S cm^{-1}, at fully hydrated state and room temperature), and 2) all the AAEMs exhibited substantially lowered conductivities at lower relative humidities; this is undesirable for the anticipated application in alkaline membrane fuel cells, where operation with low humidity gases is considered necessary. The case for development of AAEMs with conductivities that are less sensitive to humidity is therefore highlighted.

The stability of the fixed cationic site of polyelectrolytes in alkaline conditions is a concern due to nucleophilic attack by anions. Nucleophilic attack of the cation site on polymeric AAEMs is a major obstacle to achieve long term stability. Anionic fuel cells generally use hydroxide as the conductive anion. Although the high conductivity of hydroxide is attractive, hydroxide is an extremely aggressive nucleophile and can degrade the quaternary ammonium cations on the polymer, especially at high temperature [215]. Lowering the alkalinity of the mobile anion could mitigate nucleophic degradation.

In thermodynamic aspect, a large voltage loss due to the pH difference across the membrane is predicted by theoretical calculation [216]. To depress the disadvantageous effect of pH difference between anode and cathode, elevating temperature could be helpful.

In conclusion, all of these observations indicate that there is still much room to improve ADAFC performance by developing novel materials and, on the other hand, by optimizing the operational conditions of the fuel cell. Firstly, is mandatory to develop alkaline membranes which are highly conductive, stable at elevated temperatures and soluble in certain solvents for use as an anionic ionomer binder in catalytic layers. Future work should look into a wider range of potential low cost materials and composites with novel structures and properties, presenting catalytic activity comparable to that of noble metals. The development of new catalyst systems is more likely in alkaline media because of the wide range of options for the materials support and catalyst, as compared to acidic media which offers more limited materials choice. Morever, efforts have to be addressed to meet the durability targets required for commercial application. More work is needed to optimize the operational fuel cell conditions, by achieving suitable chemical (OH^- concentration, hydroxyl/alcohol ratio in the fuel stream) and physical (temperature, pressure, flow rate) parameters.

Acknowledgments

The authors thank the Conselho Nacional de Desenvolvimento Científico e Tecnológico (CNPq, Proc. 310151/2008-2) for financial assistance to the project.

References

[1] M. Cifrain, K.V. Kordesch, in: W. Vielstich, A. Lamm, H. Gasteiger (Eds.), Handbook of Fuel Cells, vol. 1, John Wiley, 2003, p. 267.
[2] G.F. McLean, T. Niet, S. Prince-Richard, N. Djilali, Int. J. Hydrogen Energy 27 (2002) 507–526.
[3] N.M. Markovic, H. Gasteiger, P.N. Ross, J. Electrochem. Soc. 144 (1997) 1591–1597.
[4] B.B. Blizanac, P.N. Ross, N.M. Markovic, Electrochim. Acta 52 (2007) 2264–2271.
[5] K. Kordesch, V. Hacker, J. Gsellmann, M. Cifrain, G. Faleschini, P. Enzinger, R. Fankhauser, M. Ortner, M. Muhr, R.R. Aronson, J. Power Sources 86 (2000) 152–165.
[6] P. Gouérec, L. Poletto, J. Denizot, E. Sanchez-Cortezon, J.H. Miners, J. Power Sources 129 (2004) 193–204.
[7] E. Gulzow, M. Schulze, U. Gerke, J. Power Sources 156 (2006) 1–7.
[8] B.Y.S. Lin, D.W. Kirk, S.J. Thorpe, J. Power Sources 161 (2006) 474–483.
[9] M. Duerr, S. Gair, A. Cruden, J. McDonald, J. Power Sources 171 (2007) 1023–1032.

[10] K. Matsuoka, Y. Iriyama, T. Abe, M. Matsuoka, Z. Ogumi, J. Power Sources 150 (2005) 27–31.
[11] J.R. Varcoe, R.C.T. Slade, E.L.H. Yee, Chem. Commun. (2006) 1428–1429, doi:10.1039/b600838k.
[12] C.C. Yang, S.J. Chiu, W.C. Chien, J. Power Sources 162 (2006) 21–29.
[13] F. Bidault, D.J.L. Brett, P.H. Middletonc, N.P. Brandon, J. Power Sources 187 (2009) 39–48.
[14] R. Dillon, S. Srinivasan, A.S. Aricò, V. Antonucci, J. Power Sources 127 (2004) 112–126.
[15] S. Wasmus, A. Kuver, J. Electroanal. Chem. 461 (1999) 14–31.
[16] E. Antolini, J. Power Sources 170 (2007) 1–12.
[17] E. Peled, V. Livshits, T. Duvdevani, J. Power Sources 106 (2002) 245–248.
[18] A.V. Tripkovic, K.D. Popovic, B.N. Grgur, B. Blizanac, P.N. Ross, N.M. Markovic, Electrochim. Acta 47 (2002) 3707–3714.
[19] E.H. Yu, K. Scott, J. Power Sources 137 (2004) 248–256.
[20] K. Scott, E. Yu, G. Vlachogiannopoulos, M. Shivare, N. Duteanu, J. Power Sources 175 (2008) 452–457.
[21] C. Coutanceau, L. Demarconnay, C. Lamy, J.-M. Léger, J. Power Sources 156 (2006) 14–19.
[22] J.S. Spendelow, A. Wieckowski, Phys. Chem. Chem. Phys. 9 (2007) 2654–2675.
[23] B. Beden, F. Kadirgan, C. Lamy, J.M. Leger, J. Electroanal. Chem. 142 (1982) 171–190.
[24] A.V. Tripkovic, K.D. Popovic, J.D. Momcilovic, D.M. Drazic, J. Electroanal. Chem. 448 (1998) 173–181.
[25] A.V. Tripkovic, K.D. Popovic, J.D. Lovic, Electrochim. Acta 46 (2001) 3163–3173.
[26] J.S. Spendelow, P.K. Babu, A. Wieckowski, Curr. Opin. Solid State Mater. Sci. 9 (2005) 37–48.
[27] O.A. Petrii, J. Solid State Electrochem. 12 (2008) 609–642.
[28] O.A. Petry, B.I. Podlovchenko, A.N. Frumkin, H. Lal, J. Electroanal. Chem. 10 (1965) 253–269.
[29] B.R. Rauhe, F.R. McLarnon, E.J. Cairns, J. Electrochem. Soc. 142 (1995) 1073–1084.
[30] A.V. Tripkovic, S. Strbac, K.Dj. Popovic, Electrochem. Commun. 5 (2003) 484–490.
[31] R.S. Jayashree, D. Egas, J.S. Spendelow, D. Natarajan, L.J. Markoski, P.J.A. Kenisa, Electrochem. Solid State Lett. 9 (2006) A252–A256.
[32] F. Kadirgan, B. Beden, J.M. Leger, C. Lamy, J. Electroanal. Chem. 125 (1981) 89–103.
[33] M. Watanabe, S. Motoo, J. Electroanal. Chem. 60 (1975) 259–266.
[34] M. Haruta, M. Date, Appl. Catal. A 222 (2001) 427–437.
[35] M. Valden, X. Lai, D.W. Goodman, Science 281 (1998) 1647–1650.
[36] J. Luo, P.N. Njoki, Y. Lin, D. Mott, L.Y. Wang, C.J. Zhong, Langmuir 22 (2006) 2892–2898.
[37] J.H. Zeng, J. Yang, J.Y. Lee, W.J. Zhou, J. Phys. Chem. B 110 (2006) 24606–24611.
[38] X. Guo, D. Guo, X. Qiu, L. Chen, W. Zhu, Eelctrochem. Commun. 10 (2008) 1748–1751.
[39] C. Xu, R. Zeng, P.K. Shen, Z. Wei, Electrochim. Acta 51 (2005) 1031–1035.
[40] P.K. Shen, C. Xu, R. Zeng, Y. Liu, Electrochem. Solid State Lett. 9 (2006) A39–A42.
[41] J. Wang, J. Xi, Y. Bai, Y. Shen, J. Sun, L. Chen, W. Zhu, X. Qiu, J. Power Sources 164 (2007) 555–560.
[42] P. Justin, G.R. Rao, Catal. Today 141 (2009) 138–143.
[43] P.C. Biswas, M. Enyo, J. Electroanal. Chem. 322 (1992) 203–220.
[44] M. Fleshmann, K. Korinek, D. Pletcher, J. Electroanal. Chem. 31 (1971) 39–49.
[45] A. Kowal, S.N. Port, R.J. Nichols, Catal. Today 38 (1997) 483–492.
[46] M.A.A. Rahim, R.M.A. Hameed, M.W. Khalil, J. Power Sources 134 (2004) 160–169.
[47] Q. Yi, W. Huang, J. Zhang, X. Liu, L. Li, Catal. Commun. 9 (2008) 2053–2058.
[48] V.A. Kazakov, V.N. Titova, A.A. Yavich, N.V. Petrova, M.R. Tarasevich, Russ. J. Electrochem. 40 (2004) 679–682.
[49] I. Danaee, M. Jafarian, F. Forouzandeh, F. Gobal, M.G. Mahjani, Int. J. Hydrogen Energy 33 (2008) 4367–4376.
[50] M. Jafarian, R.B. Moghaddam, M.G. Mahjani, F. Gobal, J. Appl. Electrochem. 36 (2006) 913–918.
[51] I.G. Casella, T.R.I. Cataldi, A.M. Salvi, E. Desimoni, Anal. Chem. 65 (1993) 3143–3150.
[52] A. Ciszewski, Electroanalysis 7 (1995) 1132–1135.
[53] A. Ciszewski, G. Milczarek, J. Electroanal. Chem. 426 (1997) 125–130.
[54] J. Taraszewska, G. Rostonek, J. Electroanal. Chem. 364 (1994) 209–213.
[55] A.N. Golikand, M. Asgari, M.G. Maragheh, S. Shahrokhian, J. Electroanal. Chem. 568 (2006) 155–160.
[56] S.M. Golabi, A. Nozad, Electroanalysis 16 (2004) 199–209.
[57] W.S. Cardoso, V.L.N. Dias, W.M. Costa, I. de Araujo Rodrigues, E.P. Marques, A.G. Sousa, J. Boaventura, C.W.B. Bezerra, C. Song, H. Liu, J. Zhang, A.L.B. Marques, J. Appl. Electrochem. 39 (2009) 55–64.
[58] A.N. Golikand, J. Raoof, M. Baghayeri, M. Asgari, L. Irannejad, Russ. J. Electrochem. 45 (2009) 192–198.
[59] M. Avramov-Ivic, V. Jovanovic, G. Vlajnic, J. Popic, J. Electroanal. Chem. 423 (1997) 119–124.
[60] Z. Borkowska, A. Tymosiak-Zielinska, G. Shul, Electrochim. Acta 49 (2004) 1209–1220.
[61] J. Hernandez, J. Solla-Gullón, E. Herrero, A. Aldaz, J.M. Feliu, Electrochim. Acta 52 (2006) 1662–1669.
[62] H. Bunazawa, Y. Yamazaki, J. Power Sources 190 (2009) 210–215.
[63] K.S. Kumar, P. Haridoss, S.K. Seshadri, Surf. Coat. Technol. 202 (2008) 1764–1770.
[64] Z. Liu, X. Zhang, L. Hong, Electrochem. Commun. 11 (2009) 925–928.
[65] M. Wang, W. Liu, C. Huang, Int. J. Hydrogen Energy 34 (2009) 2758–2764.
[66] B. Guo, S. Zhao, G. Han, L. Zhang, Electrochim. Acta 53 (2008) 5174–5179.
[67] B. Ballarin, M.C. Cassani, E. Scavetta, D. Tonelli, Electrochim. Acta 53 (2008) 8034–8044.
[68] J.H. White, A.F. Sammells, J. Electrochem. Soc. 140 (1993) 2167–2177.
[69] V. Raghuveer, K.R. Thampi, N. Xanthopoulos, H.J. Mathieu, B. Viswanathan, Solid State Ionics 140 (2001) 263–274.
[70] H.-C. Yu, K.-Z. Fung, T.-C. Guo, W. Li Chang, Electrochim. Acta 50 (2004) 811–816.
[71] R.N. Singh, T. Sharma, A. Singh, D. Anindita, D. Mishra, S.K. Tiwari, Electrochim. Acta 53 (2008) 2322–2330.
[72] R.N. Singh, A. Singh, D. Mishra, P. Anindita, Chartier, J. Power Sources 185 (2008) 776–783.
[73] C. Xu, L. Cheng, P.K. Shen, Y. Liu, Electrochem. Commun. 9 (2007) 997–1001.
[74] Z.X. Liang, T.S. Zhao, J.B. Xu, L.D. Zhu, Electrochim. Acta 54 (2009) 2203–2208.
[75] H. Wang, C. Xu, F. Cheng, S. Jiang, Electrochem. Commun. 9 (2007) 1212–1216.
[76] A.A. El-Shafei, S.A. Abd El-Maksuod, M.N.H. Moussa, J. Electroanal. Chem. 336 (1992) 73–83.
[77] Y. Chen, L. Zhuang, J. Lu, Chin. J. Catal. 28 (2007) 870–874.
[78] Q. He, W. Chen, S. Mukerjee, S. Chen, F. Laufek, J. Power Sources 187 (2009) 298–304.
[79] L.-S. Jou, J.-K. Chang, T.-J. Twhang, I.-W. Sun, J. Electrochem. Soc. 156 (2009) D193–D197.
[80] C. Xu, P.K. Shen, J. Power Sources 142 (2005) 27–29.
[81] Y. Bai, J. Wu, J. Xi, J. Wang, W. Zhu, L. Chen, X. Qiu, Electrochem. Commun. 7 (2005) 1087–1090.
[82] C. Xu, P.K. Shen, X. Ji, R. Zeng, Y. Liu, Electrochem. Commun. 7 (2005) 1305–1308.
[83] P.K. Shen, C. Xu, Electrochem. Commun. 8 (2006) 184–188.
[84] F. Hu, C. Chen, Z. Wang, G. Wei, P.K. Shen, Electrochim. Acta 52 (2006) 1087–1091.
[85] C. Xu, P.K. Shen, Y. Liu, J. Power Sources 164 (2007) 527–531.
[86] C. Xu, Z. Tian, P.K. Shen, S.P. Jiang, Electrochim. Acta 53 (2008) 2610–2618.
[87] D. Chu, J. Wang, S. Wang, L. Zha, J. He, Y. Hou, Y. Yan, H. Lin, Z. Tian, Catal. Commun. 10 (2009) 955–958.
[88] S.R. Brankovic, J. McBreen, R.R. Adzic, Surf. Sci. 479 (2001) L363–L368.
[89] F. Vitse, M. Cooper, G. Botte, J. Power Sources 142 (2005) 18–26.
[90] V. Bambagioni, C. Bianchini, J. Filippi, W. Oberhauser, A. Marchionni, F. Vizza, R. Psaro, L. Sordelli, M.L. Foresti, M. Innocenti, ChemSusChem 2 (2009) 99–112.
[91] J.-W. Kim, S.-M. Park, J. Electrochem. Soc. 146 (1999) 1075–1080.
[92] J.-W. Kim, S.-M. Park, J. Electrochem. Soc. 150 (2003) E560–E566.
[93] D.T. Shieh, B.J. Hwang, J. Electrochem. Soc. 142 (1995) 816–823.
[94] K.P. Ta, J. Newman, J. Electrochem. Soc. 146 (1998) 3860–3874.
[95] B. Beden, I. Cetin, A. Kahyaoglu, D. Takky, C. Lamy, J. Catal. 104 (1987) 37–46.
[96] S.-Ch. Chang, Y. Ho, M.J. Weaver, J. Am. Chem. Soc. 113 (1991) 9506–9513.
[97] F. Hahn, B. Beden, F. Kadirgan, C. Lamy, J. Electroanal. Chem. 216 (1987) 169–180.
[98] P.A. Christensen, A. Hamnett, J. Electroanal. Chem. 260 (1989) 347–359.
[99] K. Matsuoka, Y. Iriyama, T. Abe, M. Matsuoka, Z. Ogumi, Electrochim. Acta 51 (2005) 1085–1090.
[100] H. Kohlmuller, J. Power Sources 1 (1976/1977) 249–256.
[101] N. Dalbay, F. Kadirgan, Electrochim. Acta 36 (1991) 353–356.
[102] F. Kadirgan, B. Beden, C. Lamy, J. Electroanal. Chem. 143 (1983) 135–152.
[103] A.A. E1-Shafei, H.M. Shabanah, M.N.H. Moussa, J. Power Sources 46 (1993) 17–27.
[104] L. Demarconnay, S. Brimaud, C. Coutanceau, J.-M. Léger, J. Electroanal. Chem. 601 (2007) 169–180.
[105] B. Beden, F. Kadirgan, A. Kahyaoglu, C. Lamy, J. Electroanal. Chem. 135 (1982) 329–334.
[106] A.A. E1-Shafei a, S.A. Abd E1-Maksoud b, A.S. Fouda, J. Electroanal. Chem. 395 (1995) 181–187.
[107] C. Jin, Y. Song, Z. Chen, Electrochim. Acta 54 (2009) 4136–4140.
[108] H. Moller, P.C. Pistorius, J. Electroanal. Chem. 570 (2004) 243–255.
[109] F. Kadirgan, E. Boulder-Charbonnier, C. Lamy, J.M. Leger, B. Beden, J. Electroanal. Chem. 286 (1990) 41–61.
[110] K. Matsuoka, Y. Iriyama, T. Abe, M. Matsuoka, Z. Ogumi, J. Electrochem. Soc. 152 (2005) A729–A731.
[111] E. Yeager, Electrochim. Acta 29 (1984) 1527–1537.
[112] T.J. Schmidt, V. Stamenkovic, P.N. Ross, N.M. Markovic, Phys. Chem. Chem. Phys. 5 (2003) 400–406.
[113] L. Geniès, R. Faure, R. Durand, Electrochim. Acta 44 (1998) 1317–1327.
[114] K.V. Ramesh, A.K. Shukla, J. Power Sources 19 (1987) 279–285.
[115] G. Couturier, D.W. Kirk, P.J. Hyde, S. Srinivasan, Electrochim. Acta 32 (1987) 995–1005.
[116] Y. Kiros, J. Electrochem. Soc. 143 (1996) 2152–2157.
[117] L. Xiong, A. Manthiram, J. Mater. Chem. 9 (2004) 1454–1460.
[118] J. Luo, P.N. Njoki, Y. Lin, L. Wang, C.J. Zhong, Electrochem. Commun. 8 (2006) 581–587.
[119] F.H.B. Lima, M.L. Calegaro, E.A. Ticianelli, Russ. J. Electrochem. 42 (2006) 1283–1290.
[120] L. Demarconnay, C. Coutanceau, J.-M. Léger, Electrochim. Acta 53 (2008) 3232–3241.

[121] F.H.B. Lima, C. Sanchez, E.A. Ticianelli, J. Electrochem. Soc. 152 (2005) A1466–A1473.
[122] T.J. Schmidt, V. Stamenkovic, M. Arenz, N.M. Markovic, P.N. Ross Jr., Electrochim. Acta 47 (2002) 3765–3776.
[123] F.H.B. Lima, J. Zhang, M.H. Shao, K. Sasaki, M.B. Vukmirovic, E.A. Ticianelli, R.R. Adzic, J. Phys. Chem. C 111 (2007) 404–410.
[124] Y.F. Yang, Y.H. Zhou, C.S. Cha, Electrochim. Acta 40 (1995) 2579–2586.
[125] L. Jiang, A. Hsu, D. Chu, R. Chen, J. Electrochem. Soc. 156 (2009) B370–B376.
[126] J. Kim, T. Momma, T. Osaka, J. Power Sources 189 (2009) 909–915.
[127] N. Furuya, H. Aikawa, Electrochim. Acta 45 (2000) 4251–4256.
[128] K. Okajima, K. Nabekura, T. Kondoh, M. Sudoh, J. Electrochem. Soc. 152 (2005) D117–120.
[129] L. Demarconnay, C. Coutanceau, J.-M. Léger, Electrochim. Acta 49 (2004) 4513–4521.
[130] R. Kotz, E. Yeager, J. Electroanal. Chem. 111 (1980) 105–110.
[131] M. Chatenet, L. Genies-Bultel, M. Aurousseau, R. Durand, F. Andolfatto, J. Appl. Electrochem. 32 (2002) 1131–1140.
[132] F.H.B. Lima, J.F.R. de Castro, E.A. Ticianelli, J. Power Sources 161 (2006) 806–812.
[133] H.K. Lee, J.P. Shim, M.J. Shim, S.W. Kim, J.S. Lee, Mater. Chem. Phys. 45 (1996) 238–242.
[134] A. Raj, K.I. Vasu, J. Appl. Electrochem. 23 (1993) 728–734.
[135] A. Verma, A.K. Jha, S. Basu, J. Power Sources 141 (2005) 30–34.
[136] J.P. Brenet, J. Power Sources 4 (1979) 183–190.
[137] K. Matsuki, H. Kamada, Electrochim. Acta 31 (1986) 13–18.
[138] L. Mao, D. Zhang, T. Sotomura, K. Nakatsu, N. Koshiba, T. Ohsaka, Electrochim. Acta 48 (2003) 1015–1021.
[139] F.H.B. Lima, M.L. Calegaro, E.A. Ticianelli, J. Electroanal. Chem. 590 (2006) 152–160.
[140] I. Roche, E. Chaınet, M. Chatenet, J. Vondrak, J. Phys. Chem. C 111 (2007) 1434–1443.
[141] M. Fukuda, C. Iida, M. Nakayama, Mater. Res. Bull. 44 (2009) 1323–1327.
[142] L. Jorissen, J. Power Sources 155 (2006) 23–32.
[143] J.C. Boivin, G. Mairesse, Chem. Mater. 10 (1998) 2870–2888.
[144] D.B. Meadowcroft, Nature 226 (1970) 847–848.
[145] O. Haas, F. Holzer, S. Müller, J.M. McBreen, X.Q. Yang, X. Sun, M. Balasubramanian, Electrochim. Acta 47 (2002) 3211–3217.
[146] R. Manoharan, A.K. Shukla, Electrochim. Acta 30 (1985) 205–209.
[147] M. Bursell, M. Pirjamali, Y. Kiros, Electrochim. Acta 47 (2002) 1651–1660.
[148] Yun-Min Chang, Pu-Wei Wu, Cheng-Yeou Wu, Yu-Chi Hsieh, J. Power Sources 189 (2009) 1003–1007.
[149] M. De Koninck, S.-C. Poirier, B. Marsan, J. Electrochem. Soc. 154 (2007) A381–A388.
[150] N. Heller-Ling, M. Prestat, J.L. Gautier, J.F. Koenig, G. Poillerat, P. Chartier, Electrochim. Acta 42 (1997) 197–202.
[151] E. Ríos, H. Reyes, J. Ortiz, J.L. Gautier, Electrochim. Acta 50 (2005) 2705–2711.
[152] A. Restovic, E. Ríos, S. Barbato, J. Ortiz, J.L. Gautier, J. Electroanal. Chem. 522 (2002) 141–151.
[153] J. Ponce, J.-L. Rehspringer, G. Poillerat, J.L. Gautier, Electrochim. Acta 46 (2001) 3373–3380.
[154] E. Ríos, S. Abarca, P. Daccarett, H. Nguyen Cong, D. Martel, J.F. Marco, J.R. Gancedo, J.L. Gautier, Int. J. Hydrogen Energy 33 (2008) 4945–4954.
[155] E. Yeager, Electrochim. Acta 29 (1984) 1527–1537.
[156] D.A. Scherson, S.L. Gupta, C. Fierro, E. Yeager, M. Kordesch, J. Eldridge, R. Hoffman, Electrochim. Acta 28 (1983) 1205–1209.
[157] Y. Kiros, O. Lindstr6m, T. Kaimakis, J. Power Sources 45 (1993) 219–227.
[158] S.Lj. Gojkovic, S. Gupta, R.F. Savinell, J. Electroanal. Chem. 462 (1999) 63–72.
[159] C. Mocchi, S. Trasatti, J. Mol. Catal. A 204–205 (2003) 713–720.
[160] R. Holze, I. Vogel, W. Vielstich, J. Electroanal. Chem. 210 (1986) 277–286.
[161] G. Koscher, K. Kordesh, J. Power Sources 136 (2004) 215–219.
[162] H. Meng, P.K. Shen, Electrochem. Commun. 8 (2006) 588–594.
[163] J. Kim, J.-E. Park, T. Momma, T. Osaka, Electrochim. Acta 54 (2009) 3412–3418.
[164] L. Jiang, A. Hsu, D. Chu, R. Chen, J. Electroanal. Chem. 629 (2009) 87–93.
[165] K. Miyazaki, N. Sugimura, K. Matsuoka, Y. Iriyama, T. Abe, M. Matsuoka, Z. Ogumi, J. Power Sources 178 (2008) 683–686.
[166] J.R. Varcoe, R.C.T. Slade, Fuel Cells 5 (2005) 187–200.
[167] E. Agel, J. Bouet, J.F. Fauvarque, J. Power Sources 101 (2001) 267–274.
[168] B. Smitha, S. Sridhar, A.A. Khan, J. Membr. Sci. 259 (2005) 10–26.
[169] B. Xing, O. Savadogo, Electrochem. Commun. 2 (2000) 697–702.
[170] H. Hou, G. Sun, R. He, Z. Wu, B. Sun, J. Power Sources 182 (2008) 95–99.
[171] H. Hou, G. Sun, R. He, B. Sun, W. Jin, H. Liu, Q. Xin, Int. J. Hydrogen Energy 33 (2008) 7172–7176.
[172] J.J. Kang, W.Y. Li, Y. Lin, X.P. Li, X.R. Xiao, S.B. Fang, Polym. Adv. Technol. 15 (2004) 61–64.
[173] F. Yi, X. Yang, Y. Li, S. Fang, Polym. Adv. Technol. 10 (1999) 473–475.
[174] Y. Xiong, Q.L. Liu, Q.H. Zeng, J. Power Sources 193 (2009) 541–546.
[175] L. Li, Y.X. Wang, J. Membr. Sci. 262 (2005) 1–4.
[176] T.N. Danks, R.C.T. Slade, J.R. Varcoe, J. Mater. Chem. 13 (2003) 712–721.
[177] R.C.T. Slade, J.R. Varcoe, Solid State Ionics 176 (2005) 585–597.
[178] J. Fang, P.K. Shen, J. Membr. Sci. 285 (2006) 317–322.
[179] H. Herman, R.C.T. Slade, J.R. Varcoe, J. Membr. Sci. 218 (2003) 147–163.
[180] J.R. Varcoe, R.C.T. Slade, Electrochem. Commun. 8 (2006) 839–843.
[181] J.R. Varcoe, Phys. Chem. Chem. Phys. 9 (2007) 1479–1486.
[182] J.R. Varcoe, R.C.T. Slade, E.L.H. Yee, S.D. Poynton, D.J. Driscoll, D.C. Apperley, Chem. Mater. 19 (2007) 2686–2693.
[183] C.-C. Yang, S.-J. Chiu, W.-C. Chien, J. Power Sources 162 (2006) 21–29.
[184] Y. Xiong, J. Fang, Q.H. Zeng, Q.L. Liu, J. Membr. Sci. 311 (2008) 319–325.
[185] Y. Xiong, Q.L. Liu, Q.G. Zhang, A.M. Zhu, J. Power Sources 183 (2008) 447–453.
[186] D. Stoica, L. Ogier, L. Akrour, F. Alloin, J.-F. Fauvarque, Electrochim. Acta 53 (2007) 1596–1603.
[187] D. Stoica, F. Alloin, S. Marais, D. Langevin, C. Chappey, P. Judeinstein, J. Phys. Chem. B 112 (2008) 12338–12346.
[188] C. Sollogoub, A. Guinault, C. Bonnebat, M. Bennjima, L. Akrour, J.F. Fauvarque, L. Ogier, J. Membr. Sci. 335 (2009) 37–42.
[189] Y. Pan, Y.H. Huang, B. Liao, G.M. Cong, J. Appl. Polym. Sci. 61 (1996) 1111–1115.
[190] L. Wu, T. Xu, D. Wu, X. Zheng, J. Membr. Sci. 310 (2008) 577–585.
[191] L. Wu, T. Xu, J. Membr. Sci. 322 (2008) 286–292.
[192] C.-C. Yang, S.-J. Chiu, K.-T. Lee, W.-C. Chien, C.-T. Lin, C.-A. Huang, J. Power Sources 184 (2008) 44–51.
[193] C.-C. Yang, C.-T. Lin, S.-J. Chiu, Desalination 233 (2008) 137–146.
[194] C.-C. Yang, Y.-J. Lee, J.M. Yang, J. Power Sources 188 (2009) 30–37.
[195] Y. Xiong, Q.L. Liu, A.M. Zhu, S.M. Huang, Q.H. Zeng, J. Power Sources 186 (2009) 328–333.
[196] Y. Wu, C. Wu, T. Xu, X. Lin, Y. Fu, J. Membr. Sci. 338 (2009) 51–60.
[197] J.R. Varcoe, R.C.T. Slade, E.L.H. Yee, S.D. Poynton, D.J. Driscoll, J. Power Sources 173 (2007) 194–199.
[198] S. Song, P. Tsiakaras, Appl. Catal. B 63 (2006) 187–193.
[199] A.Y. Leykin, O.A. Shkrebko, M.R. Tarasevich, J. Membr. Sci. 328 (2009) 86–89.
[200] Z. Ogumi, K. Matsuoka, S. Chiba, M. Matsuoka, Y. Iriyama, T. Abe, M. Inaba, Electrochemistry 70 (2002) 980–983.
[201] E.H. Yu, K. Scott, Electrochem. Commun. 6 (2004) 361–365.
[202] N. Fujiwara, Z. Siroma, S. Yamazaki, T. Ioroi, H. Senoh, K. Yasuda, J. Power Sources 185 (2008) 621–626.
[203] J. Kim, T. Momma, T. Osaka, J. Power Sources 189 (2009) 999–1002.
[204] C. Bianchini, V. Bambagioni, J. Filippi, A. Marchionni, F. Vizza, P. Bert, A. Tampucci, Electrochem. Commun. 11 (2009) 1077–1080.
[205] A.D. Modestov, M.R. Tarasevich, A.Yu. Leykin, V.Ya. Filimonov, J. Power Sources 188 (2009) 502–506.
[206] S.Y. Shen, T.S. Zhao, J.B. Xu, Y.S. Li, J. Power Sources 195 (2010) 1001–1006.
[207] Y.S. Li, T.S. Zhao, Z.X. Liang, J. Power Sources 190 (2009) 223–229.
[208] V. Bambagioni, C. Bianchini, A. Marchionni, J. Filippi, F. Vizza, J. Teddy, P. Serp, M. Zhiani, J. Power Sources 190 (2009) 241–251.
[209] Y.S. Li, T.S. Zhao, Z.X. Liang, J. Power Sources 187 (2009) 387–392.
[210] J. Prabhuram, R. Manoharan, J. Power Sources 74 (1998) 54–61.
[211] E.H. Yu, K. Scott, R.W. Reeve, L. Yang, R.G. Allen, Electrochim. Acta 49 (2004) 2443–3452.
[212] E. Antolini, L. Giorgi, A. Pozio, E. Passalacqua, J. Power Sources 77 (1999) 136–142.
[213] H. Bunazawa, Y. Yamazaki, J. Power Sources 182 (2008) 48–51.
[214] M. Cifrain, K.V. Kordesch, J. Power Sources 127 (2004) 234–242.
[215] S. Chempath, B.R. Einsla, L.R. Pratt, C.S. Macomber, J.M. Boncella, J.A. Rau, B.S. Pivovar, J. Phys. Chem. C 112 (2008) 3179–3182.
[216] Y. Wang, L. Li, L. Hu, L. Zhuang, J. Lu, B. Xu, Electrochem. Commun. 5 (2003) 662–666.